NEWS IN THIS QUARTER

GNSS RO Activities at UCAR/COSMIC

The mission of the UCAR COSMIC Program (UCAR/COSMIC) is to provide innovative and cost-effective remote sensing observations, data products, and data utilization support, focusing primarily on Global Navigation Satellite System (GNSS) techniques, to benefit scientific research, research to operations, operations, and education and training in the atmospheric and related sciences. UCAR/COSMIC has been a leader in the retrieval and scientific application of GPS radio occultation (RO) data since leading the GPS/MET RO mission in mid 1990s. *Figure 1* illustrates the geometry of the GNSS-RO technique.

UCAR/COSMIC has designed, managed, and operated the Constellation Observing System for Meteorology Ionosphere and Climate (COSMIC) mission since 2006. This has had a significant positive impact on weather forecasting and atmospheric and ionospheric research. UCAR is currently supporting NOAA and the USAF in the preparation of the upcoming COSMIC-2 operational GNSS RO mission. This article summarizes recent UCAR/COSMIC activities including status of COSMIC and other RO missions, ongoing efforts to advance neutral atmospheric retrievals, scientific applications using RO data, and the upcoming COSMIC-2 mission.

IN THIS ISSUE

Figure 1. Geometry of a GNSS radio occultation sounding.

This diagram illustrates GNSS, e.g. GPS, radio occultation geometry as the low Earth orbit (LEO) satellite orbits the Earth.

COSMIC and RO Missions of Opportunity

The Constellation Observing System for Meteorology Ionosphere and Climate/FORMOSA Satellite 3 (COSMIC/FORMOSAT-3), a joint US/Taiwan mission launched in April 2006, is a six micro-satellite constellation carrying GPS RO receivers. The neutral atmosphere profile counts per day for the entire mission are shown in *Figure 2*. Satellites FM 6, and occasionally FM 1, are still operating more than 12 years after launch and are producing between 200-600 profiles/day. FMs 2, 3, 4, and 5 are not expected to operate again. Significant operational, monitoring, and debug efforts by the NSPO, UCAR, and JPL teams have extended the COSMIC mission well beyond its design lifetime of two years!

In an effort to increase the number of RO soundings available to the research and operations communities, UCAR/COSMIC is acquiring and processing data from other missions (yielding more than 6 million RO profiles). These RO missions of opportunity include GPS/MET, CHAMP, SAC-C, METOP-A/GRAS, METOP-B/GRAS, TerraSAR-X, GRACE, C/NOFS, KOMPSAT-5, and most recently PAZ (still in development). UCAR/COSMIC has been working with NOAA and Korea's Aerospace Research Institute (KARI) to make the KOMPSAT-5 RO data available in near real-time. In mid-October 2018 the NOAA Fairbanks downlink site began to collect KOMPSAT-5 on an operational basis. The data are transferred to KARI and then to UCAR for RO retrieval processing. UCAR/COSMIC is now providing the KOMPSAT-5 RO products to NOAA's PDA system in near real-time. UCAR and NOAA are now also working with the Spanish PAZ RO mission to make routine products (~250-300 soundings/day) available to the community in near real-time in the next several months. Current missions of opportunity processed by UCAR/COSMIC and total atmospheric occultation and total ionospheric occultation counts are summarized in *Table 1*. For

Figure 2. *Daily COSMIC neutral atmosphere profile count throughout the mission. The red bars show the soundings from near real-time processing. The green bars show the soundings from post-processing, often generates more sounding profiles but lags several months behind the near real-time products. The blue bars show the soundings from re-processing, which are processed every 3 years with up-to-date software.*
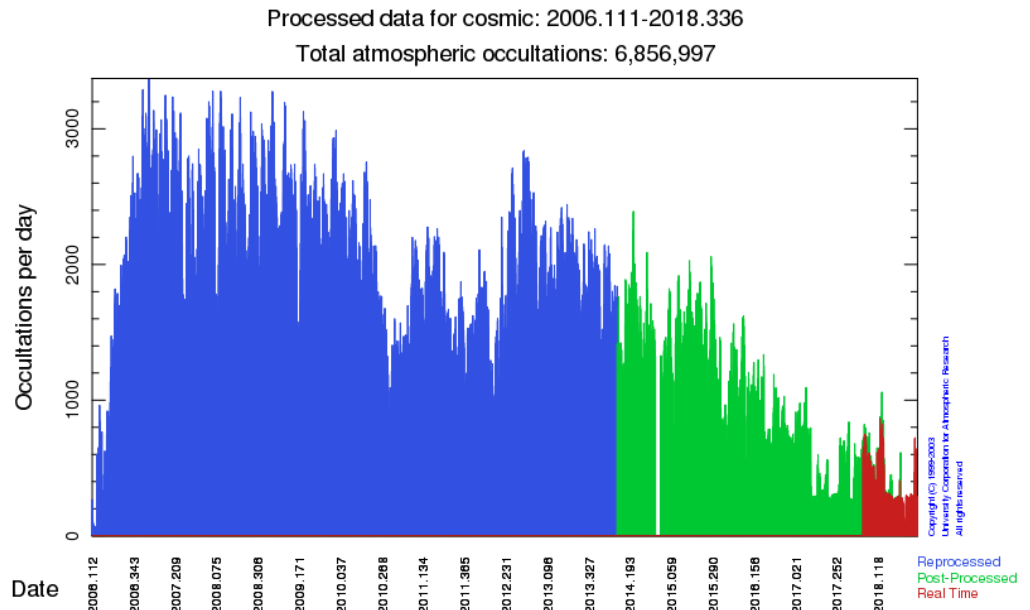
Table 1. *All missions processed by UCAR/COSMIC with total atmospheric occultation and total ionospheric occultation counts.*

Mission	Atmospheric Occultations	Ionospheric Occultations
CHAMP	468029	306318
C/NOFS	150772	0
COSMIC-1 (6 s/c) (NRT)	6860973	4597767
GPSMET	5002	0
GPSMETAS	4666	0
GRACE	555280	258283
KOMPSAT-5 (NRT)	421893	In development
METOP-A (NRT)	2369484	0
METOP-B (NRT)	1202369	0
PAZ (NRT)	44911	0
SAC-C	353756	0
Tandem-X	In development	0
TerraSAR-X	757503	0
Total	**13149727**	**5162368**

[Status December 10, 2018] [NRT = near real-time processing]

current missions, UCAR provides near real-time products where noted, and post-process all missions with latencies of about 6 weeks on a continuing basis. UCAR also periodically reprocesses the existing RO data using consistent models and data processing strategies.

RO Retrieval Improvement Efforts

UCAR/COSMIC spends considerable effort to improve the accuracy and quality control of RO retrievals in the neutral atmosphere and ionosphere. The quality of retrieved RO profiles depends on the quality of precise orbit determination solutions, removal of GNSS and LEO clock offsets, ionospheric correction, receiver open-loop tracking algorithms, and signal to noise ratio. Current efforts to improve the neutral atmospheric retrievals are listed below with lead investigators:

- Further improve precise orbit determination (Yoke Yoon)
- Further improve excess phase processing (Doug Hunt)
- Update the climatological model for statistical optimization of RO data (Janet Zeng)
- Revision of computation of local spectral width (LSW) for dynamic observational error estimation (Sergey Sokolovskiy)
- Use of back propagation for reduction of the errors of ionospheric correction (Sergey Sokolovskiy)
- Identification of the elevated tropospheric ducts from the spectrograms of radio occultation signals (Sergey Sokolovskiy)
- Development of our new 1D-Var retrieval software (Tae-Kwon Wee)
- Improve the quality control of ionospheric electron density data products (Iurii Cherniak, Doug Hunt)

- Calibration and retrieval of GNSS-Reflectometry data from NASA's CYGNSS mission (Scott Gleason, Clara Chew)

RO Science Application Efforts

The COSMIC science team conducts research on science applications in the areas of weather, climate, and space weather studies. A summary of ongoing COSMIC science application studies including their leading investigators is presented below:

- Tae-Kwon Wee is verifying the new CDAAC 1D-Var with high-resolution radiosondes
- Hailing Zhang is assessing the quality of KOMPSAT-5 bending angles
- Hailing Zhang is improving RO data impact on tropical cyclones with use of COSMIC local spectral width (LSW)
- Hailing Zhang is working on development of GPS RO observation operators in JEDI UFO in with JCSDA
- Janet Zeng is studying the representation of vertical atmospheric structures by radio occultation observations by comparison to high radiosonde profiles (Zeng et al, 2018)
- Janet Zeng is investigating the thermodynamic structures and evolution of the tropical cyclones using RO data
- Jeremiah Sjoberg is estimating error variances of RO, reanalysis, radiosondes using the N-Corner Hat method
- Jeremiah Sjoberg is estimating tropical Kelvin wave amplitudes and momentum flux from RO

- Hannah Huelsing is studying the detection and evaluation of the Saharan Air Layer using COSMIC data
- Shay Gilpin and Rick Anthes are reducing representativeness and sampling errors in radio occultation-radiosonde comparisons (Gilpin et al., 2018a/b)
- Nick Pedatella is studying the assimilation of COSMIC neutral atmospheric and ionospheric data into WACCMX+DART
- Chris Watson and Nick Pedatella have investigated the climatology of medium-scale F-region ionosphere irregularities (Watson and Pedatella, 2018)
- Iurii Cherniak is studying large-scale traveling ionospheric disturbances origin and propagation (Cherniak and Zakharenkova, 2018)
- Iurii Cherniak is evaluating IRI-2016 and NeQuick with COSMIC and Jason-2 altimeter/GPS data (Cherniak and Zakharenkova, 2018)

COSMIC-2 Status

The success of COSMIC/FORMOSAT-3 has prompted U.S. agencies (led by NOAA) and Taiwan's National Space Organization to execute a COSMIC follow-on operational mission called COSMIC-2/FORMOSAT-7 (referred to as COSMIC-2) that will put six satellites with Global Navigation Satellite System (GNSS) RO payloads into a 520 km altitude 24 degree inclination low Earth orbit (LEO). COSMIC-2 will make use of an advanced radio occultation receiver with an innovative high gain beam-forming antenna design developed at JPL, and is expected to produce at least 5,000 high quality atmospheric and ionospheric profiles per day from GPS and GLONASS signals. The expected daily RO coverage for COSMIC-2 is shown in *Figure 3*.

These high-SNR soundings from COSMIC-2 are expected to allow detection of the heights of super-refraction layers in the lower troposphere, which should positively

Figure 3. Expected daily GNSS RO occultation coverage from NOAA's COSMIC-2 mission in green. Radiosonde sites in red.
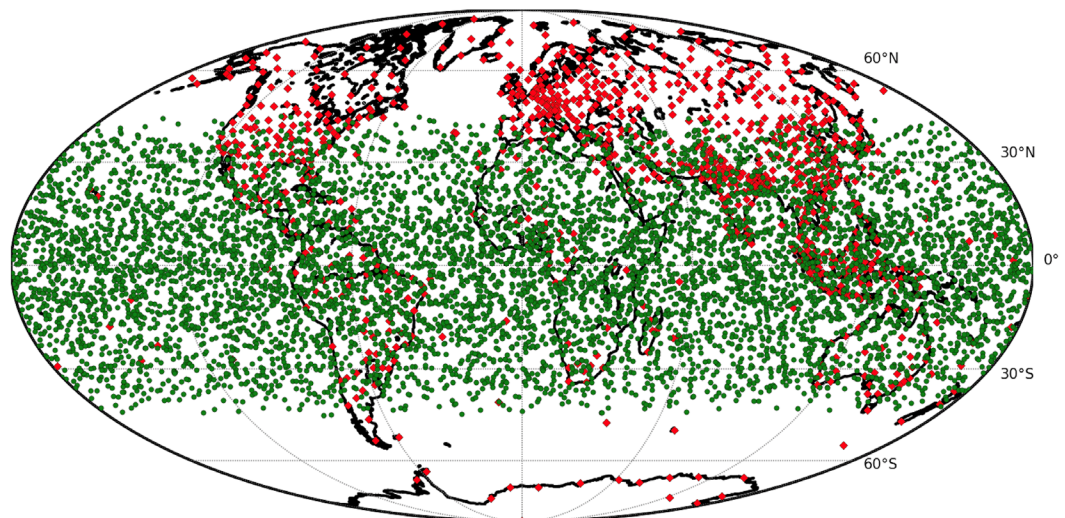
impact the assimilation of RO data into NWP models and also lead to more impactful scientific applications of RO data. COSMIC-2 products will support operational weather prediction, climate monitoring, and space weather specification and forecasting. UCAR/COSMIC is working towards a COSMIC-2 launch date that is expected to be no earlier than April 30, 2019. We are keeping our fingers crossed for a successful COSMIC-2 launch!

Author
Bill Schreiner, COSMIC Program Director, UCAR Community Programs

References

Cherniak, I., and Zakharenkova, I. (2018). Large-scale traveling ionospheric disturbances origin and propagation: Case study of the December 2015 geomagnetic storm. Space Weather, 16. https://doi.org/10.1029/2018SW001869.

Cherniak, I., and Zakharenkova, I., (2018) Evaluation of the IRI-2016 and NeQuick electron content specification by COSMIC GPS radio occultation, ground-based GPS and Jason-2 joint altimeter/GPS observations, Advances in Space Research, accepted for publication.

Gilpin, S., T. Rieckh and R.A. Anthes, 2018a: Reducing representativeness and sampling errors in radio occultation-radiosonde comparisons. Atmos. Meas. Tech., 11, 2567–2582, 2018 https://doi.org/10.5194/amt-11-2567-2018.

Gilpin, S., R. Anthes, and S. Sokolovskiy, 2018b: Sensitivity of forward-modeled bending angles to vertical interpolation of refractivity for radio occultation data assimilation. Accepted by Mon. Wea. Rev.

Watson, C., and N. M. Pedatella (2018), Climatology and characteristics of medium-scale F region ionospheric plasma irregularities observed by COSMIC radio occultation receivers, J. Geophys. Res., 123, doi:10.1029/2018JA025696.

Zakharenkova I., and I. Cherniak, (2018), Underutilized space-borne GPS observations for Space Weather monitoring, Space Weather, 16, 345–362. https://doi.org/10.1002/2017SW001756.

Zeng, Z., S. Sokolovskiy, W. S. Schreiner, and D. Hunt, (2018) Representation of vertical atmospheric structures by radio occultation observations: comparison to high radiosonde profiles, J. Atmos. Oceanic Tech. (under review)

Global Navigation Satellite Systems Radio Occultation Data Assimilation at JCSDA

The radio occultation (RO) technique was first used by NASA in probing the atmosphere of Venus in the 1960s. Although it had been suggested that the technique could be applied to detect atmospheric profiles of the Earth, it only became a feasible proposition with the deployment of Global Navigation Satellite Systems (GNSS) during the 1980s in the former Soviet Union (Vorobev and Krasilnikova 1994) and in the USA (Melbourne et al., 1994). The technique was demonstrated for the Earth atmosphere by the proof-of-concept mission GPS/MET in 1995 (Kursinski et al., 1997). The GPS/MET mission ended in 1997. Several RO missions were launched afterward. Those RO missions include: the Challenging Minisatellite Payload launched (CHAMP, 2000-2008); the Satélite de Aplicaciones Científicas-C (SAC-C, 2001-2011); the Gravity Recovery and Climate Experiment (GRACE, since 2006); the Constellation Observing System for Meteorology, Ionosphere, and Climate (COSMIC, since 2006), TerraSAR-X (since 2008), TANDEM-X (since 2010), the Communication/Navigation Outage Forecasting System Occultation Receiver for Ionospheric Sensing and Specification (C/NOFS 2008-2015); the GNSS Receiver for Atmospheric Sounding on MetOp-A (since 2006) -B (since 2012), and -C (since 2018); Radio Occultation Sounder of the Atmosphere on OceanSat-2 (since 2009), Megha-Tropiques (since 2011), the Korea Multi-Purpose Satellite-5 (KOMPSAT-5, since 2013), the Feng-Yun-3 Global Navigation Occultation Sounder (GNOS on FY-3C since 2013, and FY-3D since 2017), and the Radio Occultation and Heavy Precipitation PAZ (RHOP PAZ since 2018).

The theory of the RO technique is based on the refractive properties of the atmosphere. When a radio signal transmitted by a GPS satellite is received by the GPS receiver onboard a Low Earth Orbit (LEO) satellite, the ray path is refracted by the atmosphere and bent in the direction of increasing refractivity (i.e., toward the Earth). *Figure 1* depicts the geometry of a RO event. Note that the figure is not scaled as the GPS satellite is on an orbit of about 20,200 km, while the LEO is moving around the Earth at about 800 km. It usually takes around one minute to sample ray paths at high frequency with tangent heights between 60 km altitude and the surface. During an occultation, the ray perigee, which is also the ray point tangent to the Earth, can drift around 100 km in the horizontal (Healy et al., 2001). As the waves travel to the Earth, the ionosphere causes a bending of the rays, but its effect is frequency dependent and, using the two frequencies of the GPS signal, this effect can be corrected. Bending in the ionosphere is proportional to the total electron content present along the ray, and GNSS-RO provides important observational data of the ionosphere as well.

Figure 1. Geometry of a RO (main panel) with illustration of the atmospheric refraction (top left panel). n = c/v is the refractivity index of the medium, v is the speed of light in the medium, and c is the speed of light in the vacuum (From Zou et al. 1999).
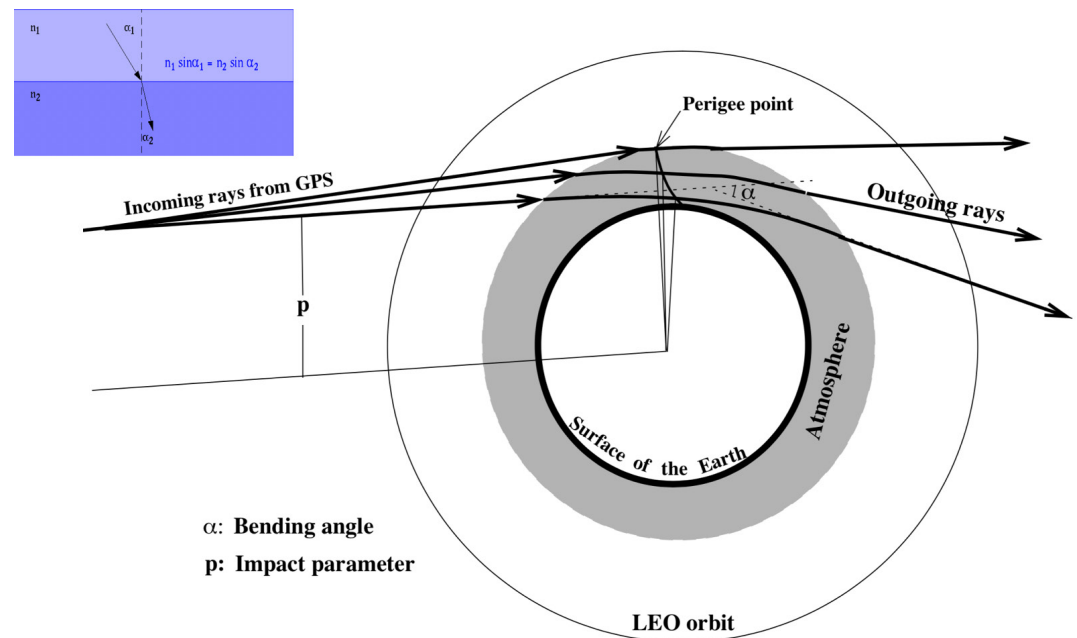
If horizontal refractivity gradients are weak near the tangent point, each ray can be characterized by two key parameters: the bending angle α , which measures how much the ray connecting the two satellites deviates from a straight line, and the impact parameter p, which measures how close the ray gets to the Earth. Those two key parameters can be retrieved from the excess phase measured by the LEO receiver using precise orbit determination. This excess phase results from the combined effects of the additional path due to the ray curvature and the presence of the atmosphere along the ray, which slows down the electromagnetic propagation. Assuming furthermore that atmospheric refractivity only varies vertically, the Abel transform, an exact mathematical inversion, can be applied to bending angles to provide the vertical refractivity at tangents points. When additional information is available, inversion techniques can then be used to retrieve temperature or humidity profiles.

Bending angle, however, is the quantity that is assimilated in Numerical Weather Prediction (NWP) models.

Compared to other satellite observations like radiances, GNSS-RO data are of a much higher vertical resolution (~1 km). While it's difficult to define the horizontal resolution due to the integral nature of the limb sounding, Anthes et al., 2000 estimated this scale to be about 300 km around the tangent point. The authors pointed out the consistency between the GNSS-RO resolved horizontal and vertical scales, whose ratio (~300) is close to Lindzen and Fox-Rabinovitz (1989) recommendations for an ideal observing system at mid-latitude. Since GNSS-RO primary observable is a Doppler shift in the L-band, the technique is not susceptible to calibration and instrument drift, nor it is sensitive to clouds, aerosols, or light precipitation. Heavy precipitations can impact navigation transmission, and research is now conducted to extract precipitation

measurements from RO polarized signals. Due to the presence of refractivity gradients near the Earth surface that can impede electromagnetic propagation, the GNSS-RO technique performs best above 8 km and below 40 km, above which residual errors from ionospheric correction can pollute the signal.

The launch in 2006 of the COSMIC mission marked a new era for GNSS-RO science. While previous single-satellite missions were providing about 300 soundings per day, the simultaneous deployment of a constellation of six satellites was able to supply nearly 3,000 profiles per day. Intense efforts at NWP centers have been dedicated to develop capabilities to assimilate GNSS-RO observations. The UK Met office was the first operational center to assimilate GNSS-RO data for its operations on September 26, 2006 (Rennie 2010), it was quickly followed by ECMWF that same year (Healy and Thépaut 2006). GNSS-RO data assimilation became operational at NCEP and Météo-France in 2007 (Cucurull and Derber 2008), at Environment Canada and JMA in 2009 (Aparicio et al., 2008, Seko et al., 2009), at DWD in 2010 (Anlauf et al., 2011), and at the US Navy in 2011. Both ECMWF and NASA have been assimilating GNSS-RO observations for the needs of their ERA and MERRA re-analysis projects, starting with CHAMP observations as early as 2001.

The assimilation of GNSS-RO data had a clear statistically beneficial impact on all variables, as measured by radiosonde fit, on 1- to 5-day forecast in the upper troposphere and stratosphere, particularly in the southern hemisphere. GNSS-RO consistently ranks in the top five most contributing observation systems to forecast error reduction, with one of the highest impacts per observation. Most importantly, it was found that the assimilation of GNSS-RO data significantly reduces model temperature biases; and therefore, can be used as reference observation in bias correction procedures, like variational bias correction, that are applied to satellite radiances before assimilation.

The JCSDA has been involved early on in the assimilation of GNSS-RO observations at NCEP (Cucurull et al., 2007) and is closely working with its partner agencies on transitioning to operations new platforms whenever they become available (see Dutta et al. article in this newsletter). This includes the preparation for the launch in 2019 of COSMIC-2, a series of six satellites equipped with new receivers able to track navigation signals deep in the troposphere (see Schreiner et al. article in this newsletter). The JCSDA supports NOAA's Commercial Weather Data Products enterprise and assists STAR in the evaluation of GNSS-RO data provided by the private sector. The Joint Center is also leading the work to integrate all GNSS-RO observation operators currently in use at its partner agencies into the Joint Efforts for Data assimilation Integration (JEDI) system. A code sprint was held in August 2018 with the participation of ECMWF to accelerate the incorporation of those observation operators in JEDI (See Shao et al. article in this newsletter). The JCSDA's activities also extends to the development of new algorithms. The main efforts are related to

better characterize observational errors and devise quality control procedures that can account for the presence of strong refractivity gradients (see Ho et al., Ruston et al., and Zhang et al. articles in this newsletter).

Authors

François Vandenberghe (JCSDA), Hui Shao (JCSDA), Suryakanti Dutta (JCSDA), Hailing Zhang (COSMIC & JCSDA), Ben Ruston (NRL), Will McCarty (NASA/GMAO), Shu-Peng Ho (NOAA/NESDIS), Lidia Cucurull (NOAA/AOR), and James Yoe (JCSDA).

References

Anthes R., C. Rocken,   Y.-H. Kuo, 2000: Application of COSMIC to Meteorology and Climate. Terr. Atmos. Oceanic Sci., 11-1, 115–156, doi: 10.3319/ TAO.2000.11.1.115(COSMIC).

Anlauf, H., D. Pingel, and A. Rhodin, 2011: Assimilation of GPS radio occultation data at DWD. Atmos. Meas. Tech., 4, 1105– 1113, doi:10.5194/amt-4-1105-2011.

Aparicio, J. M., and G. Deblonde, 2008: Impact of the assimilation of CHAMP refractivity profiles in Environment Canada global forecasts. Mon. Wea. Rev., 136, 257– 275, doi:10.1175/ 2007MWR1951.1.

Cucurull, L., and J. C. Derber, R. Treadon, and R. J. Purser, 2007: Assimilation of Global Positioning System radio occultation observations into NCEP's Global Data Assimilation System. Mon. Wea. Rev., 135, 3174–3193

Cucurull and J. C. Derber, 2008: Operational implementation of COSMIC observations into the NCEP's Global Data Assimilation System. Wea. Forecasting, 23, 702–711, doi:10.1175/2008WAF2007070.1.

Healy S., D. Lowe, D. Johnson, D. Offiler, and J. Haase, Review of airborne radio occultation techniques and meteorological measurements made from civil aircraft. Met Office Technical Note. 65 pp. 2001.

Healy, S. B., and J.-N. Thépaut, 2006: Assimilation experiments with CHAMP GPS radio occultation measurements. Quart. J. Roy. Meteor. Soc., 132, 605–623, doi:10.1256/ qj.04.182.

Kursinski, E. R., G. A. Hajj, K. R. Hardy, J. T. Schofield, and R. Linfield, 1997: Observing Earth's atmosphere with radio occultation measurements. J. Geophys. Res., 102, 23429–23 465, doi:10.1029/97JD01569.

Lindzen, R. S., and M. Fox-Rabinovitz, 1989: Consistent vertical and horizontal resolution. Mon. Wea. Rev., 117, 2575-2583.

Melbourne, W. G., and Coauthors, 1994: The application of spaceborne GPS to atmospheric limb sounding and global change monitoring. Jet Propulsion Laboratory Publ. 94-18, 142 pp.

Rennie, M. P., 2010: The impact of GPS radio occultation assimi- lation at the Met Office. Quart. J. Roy. Meteor. Soc., 136, 116– 131, doi:10.1002/qj.521.

Seko, H., Y. Shoji, M. Kunii and Y. Aoyama, 2009: Impact of the CHAMP occultation data on the rainfall forecast. Data Assimilation for Atmospheric, Oceanic and Hydrologic Applications, 1, 197-218.

Vorobev, V. V., and T. G. Krasilnikova, Estimation of the accuracy of the atmospheric refractive index recovery from Doppler shift measurements at frequencies used in the NAVSTAR system, Phys. Atmos. Ocean, 29, 602-609, 1994.

Zou X., F. Vandenberghe, B. Wang, M.E. Gorbunov, Y.H. Kuo, S. Sokolovskiy, J.C. Chang, G.G. Sela and R. Anthes: A raytracing operator and its adjoint for the use of GPS/MET refraction angle measurements. J. Geophys. Res., Vol 104, No D18, 22, 301-22,318. 1999. DOI: 10.1029/1999JD900450.

Improving the Impact of Radio Occultation Observations on Numerical Forecasts of Tropical Cyclones

Introduction

The Global Positioning System (GPS) Radio Occultation (RO) is an active remote sensing technique, which is complementary to passive microwave and infrared sounders and microwave imagers. Since its launch in 2006, Constellation Observing System for Meteorology, Ionosphere and Climate (COSMIC) RO data have been assimilated by the National Centers for Environmental Prediction (NCEP; Cucurull et al., 2013), the European Centre for Medium-Range Weather Forecasts (ECMWF; Healy and Thépaut 2006), and other global numerical weather prediction (NWP) centers in their operational systems. The high accuracy, precision, and small biases (Anthes, 2011) make RO observations useful in calibrating microwave, infrared sounding systems, as well as radiosondes (Anthes, 2011; Ho et al., 2019). Because RO data can be assimilated without bias corrections, they can be considered "anchor references" in both NWP and climate reanalysis (e.g., Poli et al., 2010; Cucurull et al., 2014; Aparicio and Laroche, 2015), preventing the model from drifting to its own biased climate. All the centers had shown positive impacts of the COSMIC RO data on global forecasts (Anthes, 2011; Ho et al., 2019). The primary impact of RO data in global NWP systems is between 7- and 35-km altitudes (Poli et al., 2010).

In addition to their positive impact on global NWP, RO data are also useful in improving the moisture analysis for extreme weather predictions using regional forecast models. In this paper, we review several studies showing the impact of RO observations on improving the water vapor analysis in moist tropical and subtropical environments. We also summarize some promising recent results of tropical cyclone forecasts using a new Dynamic Bending Angle Observation Error (DBAOE) specification in the data assimilation process (Zhang et al., 2019). In the DBAOE specification, the error of individual RO bending angles is estimated based on the local spectral width (LSW) of the RO sounding rather than using statistics to define the errors of the bending angles. The use of DBAOE allows for greater impact of the more accurate observations and less impact of the observations with greater errors compared to the use of statistical error estimates. While these results are preliminary and need to be verified by more studies using operational NWP models, they are promising in that they show the potential of RO observations to make a larger positive impact in the forecasts of tropical cyclones and other severe convective phenomena.

Tropical Cyclone Predictions

There have been a number of case studies that have examined the impact of RO observations on NWP forecasts of tropical cyclones (e.g., Chen et al., 2015 and references therein). These studies of have shown that RO data improve the tropical storms' track, intensity, and rainfall forecasts.

Hsiao et al. (2012) considered the effect of how RO and other data were assimilated in Weather Research and Forecast models (WRF) on 78 typhoon forecasts in 2008 (Sinlaku, Hagupit, and Jangmi). They showed that both an outer loop and partial cycling approach produces the largest improvement in the typhoon track forecast. The outer loop cycling includes more observations, especially RO observations distant from the typhoon center, and thus improves the analysis over the western North Pacific, which is crucial in determining the storm track.

A few studies have shown that RO observations can make the difference between model cyclogenesis and non-cyclogenesis. Liu et al. (2012) showed that when RO refractivity was assimilated using a non-local quasi-excess phase operator, moisture in the troposphere was enhanced, leading to more accurate genesis and intensification of Hurricane Ernesto (2008). Ernesto did not develop in model forecasts without RO observations, but with RO observations cyclogenesis occurred as observed. The key difference was the RO impact on increasing water vapor in the lower troposphere.

Another tropical cyclone genesis study by Kuo et al. (2016) showed a dramatic effect on WRF predictions of the genesis of Typhoon Nuri (2008), which formed over the Western Pacific Ocean at 1800 UTC 16 August 2008. Forecasts from 1800 UTC 14 August 2008 with either the ECMWF or NCEP global

analysis failed to predict the genesis of Nuri. Using a non-local observation operator (Sokolovskiy et al., 2005a,b), they performed a 3-day data assimilation with and without RO data, starting at 1800 UTC 11 to 1800 UTC 14 August 2008. *Figure 1* shows the dramatic effect of the RO observations on the precipitable water fields. As in the Ernesto case, the RO observations corrected an overly dry model troposphere and the result was a correct prediction of cyclogenesis with the assimilation of the RO observations. Kuo et al., (2016) further analyzed ten typhoons over the North Western Pacific and found that the probability of cyclogenesis detection could be doubled with RO data.

Tropical Cyclone Forecast Experiments Using a Dynamic Bending Angle Observation Error

An important aspect of data assimilation in NWP models is the estimation of the errors of the observations. Observations with small errors are given greater weight in the analysis than observations with larger errors. In the past, the errors of RO bending angles (BA) have been estimated using a statistical approach in which the errors are specified as a function of height based on RO error statistics (e.g., Ruston, 2019). However, the errors of BA vary greatly among individual RO profiles because of variations in signal-noise-ratio (SNR) and atmospheric conditions, such as large vertical refractivity gradients or violations of the assumption of spherical symmetry in the Abel retrieval of BA. Thus, the errors of some BA profiles are much larger and some are much smaller than the statistical estimate. A procedure that estimates the errors of each individual RO profile, which would allow varying impact based on the error, seems intuitively appealing.

Very recent data assimilation studies using estimates of individual RO BA based on the local LSW of individual observations have been reported by Liu et al. (2018) and Zhang et al. (2019). The LSW is illustrated in *Figure 2*.

Figure 1. Sea level pressure, boundary layer winds, and precipitable water after three days of assimilation with and without RO data (Kuo et al., 2016).
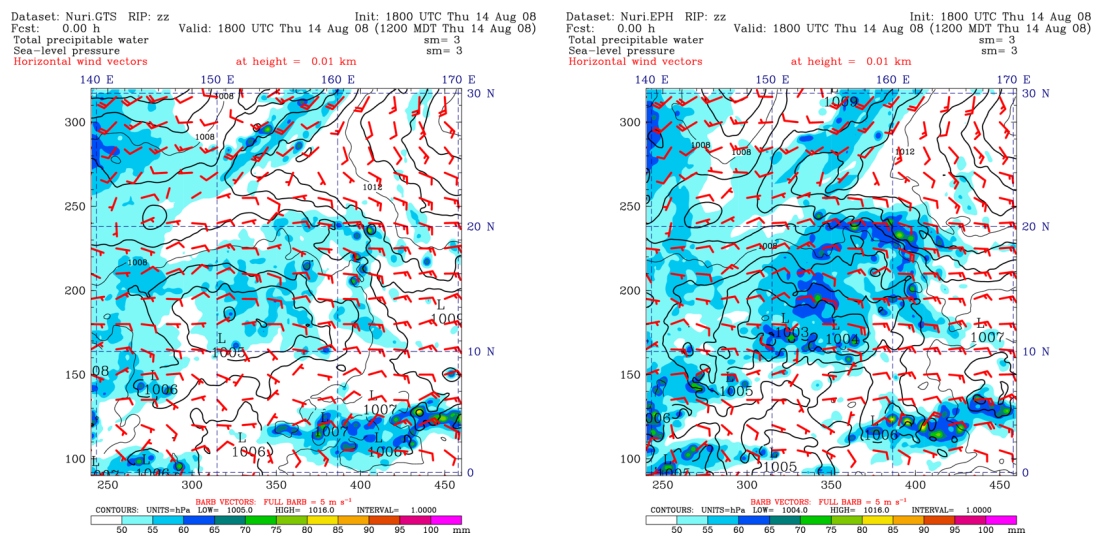
Figure 2. (a) normed local power spectrum at 3.75 km impact height for a tropical RO sounding, and (b) retrieved bending angle (red) and corresponding LSW/2 (blue) profiles. (adapted from Figure 1 of Zhang et al., 2019).
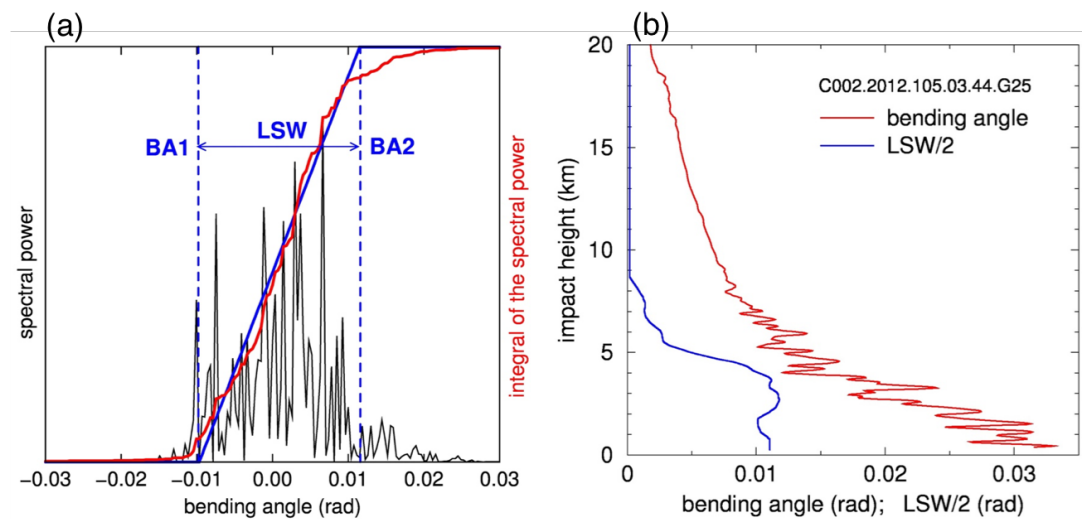
The accurate estimation of individual BAOE may be most important for improving the analysis of water vapor in the lower troposphere, where the variation of BA errors is greatest (Zhang et al., 2019). To demonstrate how COSMIC RO data with the knowledge of available LSW-based BAOE can improve track and intensity prediction, Zhang et al., (2017) considered the impact of LSW-based RO DBAOEs in forecasts of Typhoon Sinlaku (2018). They used the operational version of the NCEP GSI and GFS and included all other observations in their experimental forecasts. The LSW at each level of each RO profile is provided by the COSMIC Data Analysis and Archive Center (CDAAC, https://cdaac-www.cosmic.ucar.edu/).

Figure 3 shows the sensitivity of forecasts of Sinlaku to how the BA errors are specified in the data assimilation. For these experiments, the assimilation of BA with the statistical error specification (CTRL) actually degrades the forecast tracks compared to an experiment that excludes RO observations entirely (NORO), suggesting that BA with errors larger than the statistical specification are being given too much weight in the Control assimilation. Using the DBAOE specification of LSW/2 (DYNE) improves the forecasts compared to the Control and the NORO forecasts. Using a lower estimate of the dynamic errors in DYNEL, which gives higher weight to the most accurate RO observations, makes an even a greater positive impact. In these cases, use of the DBAOEs improves the forecasts of the fields of temperature, moisture, and wind in the storm's environment and thus improves the track forecasts. This experiment clearly shows the sensitivity of the forecasts to the specification of RO errors in the data assimilation.

Summary and Looking Ahead to COSMIC-2
In this paper, we summarized the impact of assimilating COSMIC RO observations on tropical cyclones. In a number of case studies, the inclusion of RO observations improves the track and intensity forecasts of tropical cyclones. In a few cases, RO observations made the difference between genesis and non-genesis of tropical

Figure 3. The mean TC track prediction error. In the reference case (DYNE), the DBAOE equals to the LSW/2. A lower estimate (DYNEL) of 0.5 times the reference is also tested. The control (CTRL) used the current NCEP pre-defined statistical DBAOE. (Zhang et al., 2017).
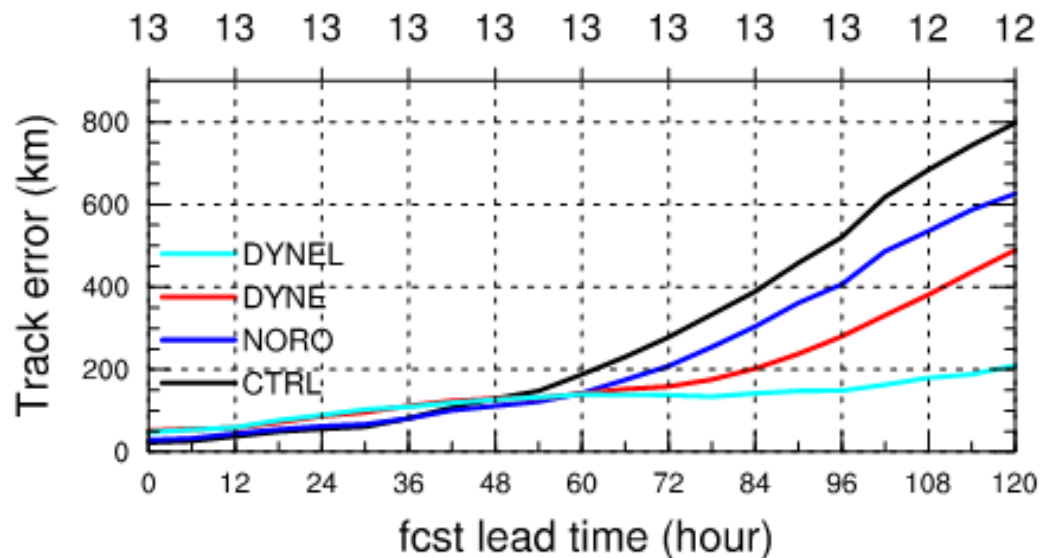
cyclones. In these cases, the assimilation of RO observations increases the water vapor content in analyses that are too dry to begin with and the resulting improved analysis leads to more accurate forecasts.

In addition, preliminary experiments using a dynamic method to estimate the errors of individual RO observations based on the LSW of the profile instead of statistical estimate of the error show promising result. In these experiments, the error of each RO observation is estimated by the LSW at the level of the observations. In the data assimilation process, therefore, more accurate (smaller LSW) RO observations are given greater weight in the analysis. Forecast experiments using the NCEP GFS/GSI system with Typhoon Sinlaku (2008) showed a large sensitivity to how the RO errors were specified, with the dynamic method of estimating the errors of individual RO sounding showing significantly improved forecasts compared to the use of statistical estimate of RO error.

COSMIC-2 (Schreiner, 2019, this issue), scheduled to be launched in 2019, promises even greater positive impact on heavy rainfall and tropical cyclone events. The COSMIC-2 constellation consists of six satellites at 24° inclination, which will enhance observations in the equatorial region over what is currently being collected with COSMIC. COSMIC-2 will carry a JPL Tri-GNSS (TriG) RO receiver and will collect more soundings per receiver by adding the European Galileo system and Russia's GLONASS tracking capability, which will produce a significantly higher spatial and temporal density of profiles in the tropics. With the advanced TriG receiver and improved antenna system, COSMIC-2 is expected to produce many more soundings in the tropics with higher accuracy and a greater number of soundings penetrating into the tropical planetary boundary layer. These observations have the potential to increase the impact of RO observations on tropical cyclone forecasts and an opportunity to study in greater detail the

impact of dynamic error specification of RO data in NWP data assimilation.

Authors

Shu-peng Ho, NESDIS/STAR/SMCD
shu-peng.ho@noaa.gov

Richard A. Anthes, COSMIC Program Office, UCAR
anthes@ucar.edu

Hailing Zhang, COSMIC Program Office, UCAR
hailingz@ucar.edu

Shu-Ya Chen, (GPS Science and Application Research Center, National Central University, Taiwan)
shuyachen@ncu.edu.tw

References

Anthes, R. A., 2011: Exploring Earth's atmosphere with radio occultation: contributions to weather, climate and space weather, *Atmos. Meas. Tech.*, 4, 1077-1103, doi:10.5194/amt-4-1077-2011.

Aparicio, J.M. and S. Laroche, 2015: Estimation of the Added Value of the Absolute Calibration of GPS Radio Occultation Data for Numerical Weather Prediction. *Mon. Wea. Rev.*, 143, 1259–1274, https://doi.org/10.1175/MWR-D-14-00153.1

Chen, Y.C., M.E. Hsieh, L.F. Hsiao, Y.-H. Kuo, M.J. Yang, C.-Y. Huang and C.S. Lee, 2015: Systematic evaluation of the impacts of GPSRO data on the prediction of typhoons over the northwestern Pacific in 2008-2010. *Atmos. Meas. Tech.* 8, 2531-2542. Doi:10.5194/amt-8-2531-2015

Cucurull, L., J. C. Derber, and R. J. Purser, 2013: A bending angle forward operator for global positioning system radio occultation measurements, J. *Geophys. Res. Atmos.*, 118, 14–28, doi:10.1029/2012JD017782.

Cucurull, L., R.A. Anthes and L.L. Tsao, 2014: Radio occultation observations as anchor observations in numerical weather prediction models and associated reduction of bias corrections in microwave and infrared satellite observations. J. Atmos. Oceanic. Technol., 31, 20-32, doi:10.1175/JTECH-D-13-00059.1

Healy, S. B. and J. Thépaut, 2006: Assimilation experiments with CHAMP GPS radio occultation measurements. *Quart. J. Roy. Meteor. Soc.*, 132: 605-623. doi:10.1256/qj.04.182

Ho, S.-P., R. A. Anthes, C. O. Ao, S. Healy, A. Horanyi, D. Hunt, A. J. Mannucci, J.-Y. Liu, N. Pedatella, W. J. Randel, A. Simmons, A. Steiner, F. Xie, X. Yue, Z. Zeng, 2019: The COSMIC/FORMOSAT-3 Radio Occultation Mission after 12 years: Accomplishments, Remaining Challenges, and Potential Impacts of COSMIC-2, *Bulletin of the American Meteorological Society* (submitted).

Hsaio, Ling-Fang, Der-Song Chen, Ying-Hwa Kuo, Yong-Run Guo, Tien-Chiang Yeh, Jing-Shan Hong, Chin-Tzu Fong, and Cheng-Shang Lee, 2012: Application of WRF 3DVAR to Operational Typhoon Prediction in Taiwan: Impact of Outer Loop and Partial Cycling Approaches. *Wea. Forecasting*, 27(5), 1249-1263, doi:10.1175/WAF-D-11-00131.1.

Kuo, Y.-H., S. Y. Chen and T. J. Galarneau Jr, 2016: Impact of GPS Radio Occultation Data on the Prediction of Tropical Cyclogenesis. Joint 30th Conference on Hydrology and the Special Sessions on US-International Partnership, 98th AMS annual meeting, 11–15 January 2016, New Orleans, LA.

Liu, H., J. Anderson, and Y.-H. Kuo, 2012: Improved Analyses and Forecasts of Hurricane Ernesto's Genesis Using Radio Occultation Data in an Ensemble Filter Assimilation System. *Mon. Wea. Rev.*, 140, 151-166, doi:10.1175/MWR-D-11-00024.1.

Liu, H., Y.-H. Kuo, S. Sokolovskiy, X. Zou, Z. Zeng, L.-F. Hsiao, and B.C. Ruston, 2018: A Quality Control Procedure Based on Bending Angle Measurement Uncertainty for Radio Occultation Data Assimilation in the Tropical Lower Troposphere. J. *Atmos. Oceanic Technol.*, 35, 2117 – 2131, doi:10.1175/ JTECH-D-17-0224.1, 2117-2131.

Poli, P., S.B. Healy, and D.P. Dee, 2010: Assimilation of Global Positioning System radio occultation data in the ECMWF ERA-Interim reanalysis. *Quart. J. Roy. Meteor. Soc.*, 136: 1972-1990, doi: 10.102/qj.172.

Ruston, B., 2019: Consideration for GNSS-RO ending angle observation error. *JCSDA Quarterly*, 62, Winter 2019 (this issue).

Schreiner, W.S., 2019: GNSS-RO Activities at UCAR/COSMIC. *JCSDA Quarterly, 62*, Winter 2019 (this issue).

Sokolovskiy, S. , Y.-H. Kuo, and W. Wang, 2005a: Assessing the accuracy of a linearized observation operator for assimilation of radio occultation data: Case simulations with a high-resolution weather model. Mon. Wea. Rev., 133, 2200–2212, https://doi.org/10.1175/MWR2948.1.

Sokolovskiy, S. , Y.-H. Kuo, and W. Wang ,2005b: Evaluation of a linear phase observation operator with CHAMP radio occultation data and 2130 JOURNAL OF ATMOSPHERIC AND OCEANIC TECHNOLOGY VOLUME 35 high-resolution regional analysis. Mon. Wea. Rev., 133, 3053–3059, https://doi.org/10.1175/MWR3006.1.

Zhang, H., S.-P. Ho, S. Sokolovskiy, Y.-H. Kuo, and R.A. Anthes, 2019: Impact of dynamic error specification on the assimilation of GPS RO bending angles for global numerical weather prediction. *Atmospheric Chemistry and Physics*. (to be submitted in early 2019).

Zhang, H., S.-P. Ho and Y.-H. Kuo, 2017: Impact of RO dynamic observation error estimate on NWP using the NCEP GFS/GSI System. AGU Fall meeting, 11-15 December 2017, New Orleans, LA.

Considerations for GNSS-RO Bending Angle Observation Error

The global navigation satellite systems are used to provide radio occultations (GNSS-RO). One of the first successful implementations of a one-dimensional bending angle operator was performed at the European Centre for Medium-Range Weather Forecasts (ECMWF) by Healy and Thépaut (2006). The assimilation of bending angle is now a common practice among global numerical weather prediction centers as they have demonstrated both positive impact on forecasts and in the fit to other observations (Anthes et al., 2008; Cucurull and Derber, 2008; and Healy, 2008). The horizontal scales to which the measurement are sensitive is often quite broad, roughly 200 km, and consequently in the lower troposphere the measurements are susceptible to horizontal gradients particularly those in moisture (Chen et. al, 2011). Due to this consideration, there is general consistency among centers on the performance of the GNSS-RO bending angles with the best use of and fits to the observations occurring between 8-30 km. Though the measurements are often used up to a height of 60 km, the measurement itself approaches the noise floor and the signal-to-noise ratio degrades. From these general guidelines, a bending angle error model shows large values near the surface, a reduction around the tropopause, and a relatively constant error upwards until the measurement begins to approach the noise floor of the instrument.

A simple GNSS-RO bending angle error model will exhibit those characteristics, which are obtained from the assimilation system itself in fit to the background forecast or analysis. Global fits of the observation minus the background (O-B) and the standard deviation are available from many sources including the European Organisation for the Exploitation of Meteorological Satellites (EUMETSAT) Radio Occultation Meteorology Satellite Application Facility (ROM-SAF) near real-time page (http://www.romsaf.org/monitoring/index.php) or one from the Naval Research Laboratory (NRL) monitoring the Navy Global Environmental Model (NAVGEM) run by Fleet Numerical Meteorology and Oceanography Center (FNMOC) https://www.nrlmry.navy.mil/metoc/ar_monitor/. *Figure 1* shows examples of the bending angle assimilation monitoring for global O-B, or innovation, normalized by the bending angle simulated from the background forecast from the ROM-SAF and NRL in the left and right panels respectively for the month of October 2018. These show a general consistency in the performance of the systems. The dashed lines show the global standard deviations of the O-B, and this structure is mimicked by many centers to produce the bending angle observation error model. A simple model can be produced that has a high value at the surface, which decays linearly to an approximate global tropopause height, followed by a region of constant error in normalized bending angle with a final section of constant error in microradians. A typical conservative bending angle error model would use values of 20% at the surface, decaying linearly up to 10 km to a value of 1.5%, followed by a noise floor of 6 microradians. This is a conservative estimate that largely

Figure 1. The global mean and standard deviation of the observation minus background (O-B) for bending angle from the ROM-SAF (left) and NRL (right) for the ECMWF, UK Met Office, and NAVGEM systems for the GRAS sensor on MetOp-A for October 2018. The O-B or innovation is normalized by the value simulated from the background forecast.
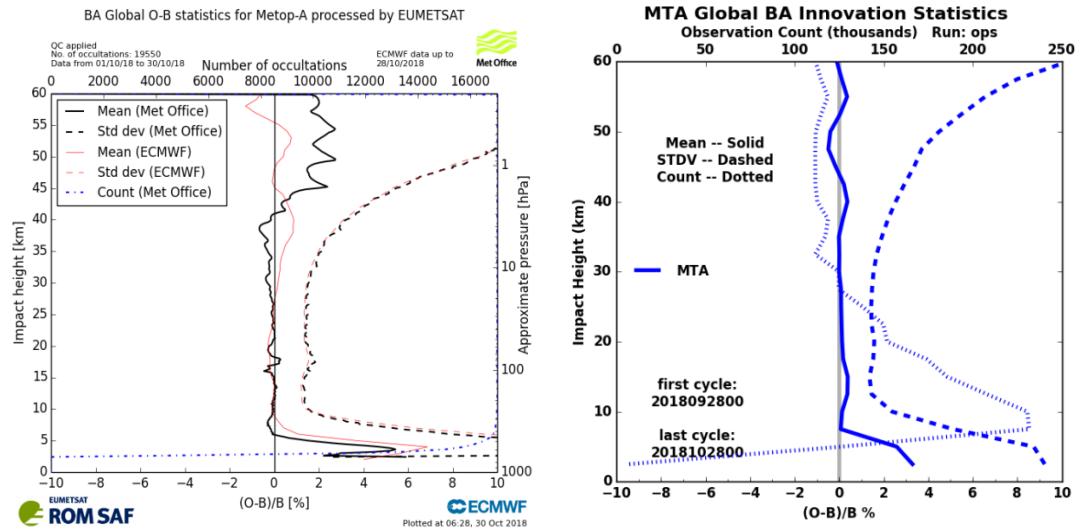
follows the O-B statistics seen in the global systems and is a good starting point when just starting out or nothing else is available.

A further update to bending angle observation error could be made to follow some of the latitudinal characteristics of the bending angle statistics. *Figure 2* shows a zonal plot of the standard deviation of the normalized O-B on the left, along with a model of bending angle error on the right. The model of bending angle error can use latitude as a predictor for parameters to mimic the standard deviations from the system. By using the cosine of the latitude to vary two values, a better fit to the observed standard deviation of O-B can be constructed. A model to fit the O-B standard deviations is created using cosine of latitude to vary: the maximum error at the surface from 25% at the Equator to two-thirds of this value or 16.67% at the poles; and second the estimate of tropopause height from 12 km at the Equator to 5.33 km at the poles.   The normalized standard deviation of O-B for all GNSS-RO sensors assimilated into NAVGEM, and the resulting normalized error profile following

such a model are shown in *Figure 2*, with the standard deviation on the left and error model on the right.

To improve the error model for bending angle, information on the uncertainty in the measurement and the environmental characteristics would be appropriate. A bending angle assimilated is a function of the impact parameter retrieved from the GNSS-RO measurements, which are a measure of the refraction of radio waves through the atmosphere that affects their phase and amplitude. This inversion is done under the assumption of local spherical symmetry of the refractivity and the process can be done using a wave optics (WO) method (e.g., Gorbunov 2002; Jensen et al., 2003). In a moist lower troposphere, strong vertical and horizontal gradients of humidity can result in multiple rays comprising the radio occultation (RO) signal having the same impact parameter, which broadens the overall width of the local power spectrum of RO signal transformed to impact parameter representation by WO methods. Gorbunov et al. (2006) first proposed the local spectral

Figure 2. The global standard deviation (left) of the observation minus background (O-B) and the observational error (right) in percent for the GRAS sensor on MetOp-A for October 2018. The bending angle is normalized by the simulated bending angle. These plots are produced by NRL and use the NAVGEM system.
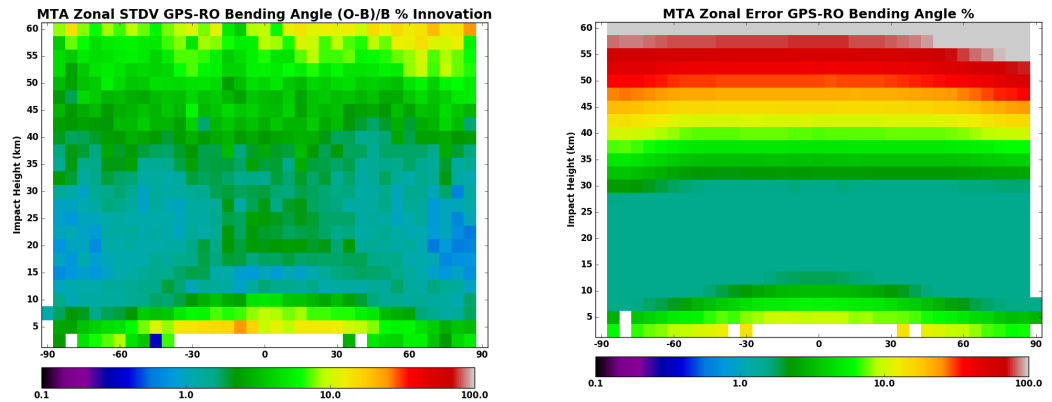
width (LSW) of WO-transformed RO signals for detection of receiver tracking errors. Sokolovskiy et al. (2007) found that the LSW of the amplitude of WO-transformed RO signals has a strong correlation with the regions of moist convection, which is responsible for large fluctuations of RO bending angles. Later, the LSW was used to determine an observational uncertainty in the bending angle (Sokolovskiy, 2014). Recently, the use of LSW has been extended to quality control and some data assimilation experiments as well (Liu et al., 2018; and Zhang this issue). The use of LSW as either a proxy for observation error or more generally to trigger an inflation of the error is an excellent tie of the physical processes behind the measurement to the assumed observation error. It is recommended that this LSW parameter always be provided for wave optic processed radio occultation data. Another straightforward physical feature that impacts the simulation and assimilation of the bending angle are the surrounding model grid points in the background humidity field. An examination of the background humidity for horizontal inhomogeneity would be a reasonable parameter to use for increasing the observation error, which may help to account for errors in representativeness of

the forward simulation. A study that looks at the relation of the background humidity horizontal variation to the O-B, as well as the observation impact could be very useful as another observation error inflation mechanism and for use when a LSW is not available with the measurement. In short, introduction of the LSW and the model background humidity inhomogeneity to the bending angle error model would be reasonable approaches to investigate and allow a reduced dependency on the ad-hoc methods of matching the global O-B standard deviation structure.

In summary, the GNSS-RO bending angles are a reliable and effective observation source for atmospheric temperature and moisture for data assimilation. There is broad consistency between global prediction centers in the performance and model fit to the observations. The observation error models used operationally though are still crude, and the data assimilation methodology remains critically sensitive to the observation error values specified. More investigation into improvement in these observation error models could prove fruitful in improving the impact of these important measurements for Earth observation.

Author

Benjamin Ruston, Naval Research Laboratory, Monterey CA

Acknowledgments

Anthes, R. A., and Coauthors, 2008: The COSMIC/FORMOSAT-3 Mission: Early results. Bull. Amer. Meteor. Soc., 89, 313–333.

Chen, S., C. Huang, Y. Kuo, and S. Sokolovskiy, 2011: Observational Error Estimation of FORMOSAT-3/COSMIC GPS Radio Occultation Data. *Mon. Wea. Rev.*, 139, 853–865, https://doi.org/10.1175/2010MWR3260.1

Cucurull, L. and J. C. Derber, 2008: Operational implementation of COSMIC observations into NCEP's global data assimilation system. *Wea. Forecasting*, 23, 702-711.

Gorbunov, M. E., 2002: Canonical transform method for processing radio occultation data in the lower troposphere. *Radio Sci.*, 37(5), 1076, doi:10.1029/2000RS002592.

Gorbunov, M. E., K. B. Lauritsen, A. Rhodin, M. Tomassini, and L. Kornblueh, 2006: Radio holographic filtering, error estimation, and quality control of radio occultation data. J. *Geophys. Res.*, 111, D10105, doi:10.1029/2005JD006427.

Healy, S.B. and J.-N. Thépaut, 2006: Assimilation experiments with CHAMP GPS radio occultation measurements. *Q. J. R. Meteorol. Soc.*, 132, 605-623.

Healy, S. B., 2008: Forecast impact experiment with a constellation of GPS radio occultation receivers. *Atmos. Sci. Lett.*, 9, 111–118.

Jensen, A. S., M. S. Lohmann, H. Benzon, and A. S. Nielsen, 2003: Full spectrum inversion of radio occultation signals. *Radio Sci.*, 38(3), 1040, doi:10.1029/2002RS002763.

Liu, H., Y.-H. Kuo, S. Sokolovskiy, X. Zou, Z. Zeng, L.-F. Hsiao, and B. Ruston, 2018: A quality control procedure based on bending angle measurement uncertainty for radio occultation data assimilation in the tropical lower troposphere, J. *Atmos. and Ocean. Tech.*, doi:10.1175/JTECH-D-17-0224.1.

Sokolovskiy, S. V., C. Rocken, D. H. Lenschow, Y.-H. Kuo, R. A. Anthes, W. S. Schreiner, and D. C. Hunt, 2007: Observing the moist troposphere with radio occultation signals from COSMIC, Geophys. Res. Lett., doi:10.1029/2007GL030458.

Sokolovskiy, S., 2014: Improvements, modifications, and alternative approaches in the processing of GPS RO data. Presentation at ECMWF/ROMSAF Workshop on Application of GPS Radio Occultation Measurements, Reading, UK, June 16-18, 2014. https://cdaac-www.cosmic.ucar.edu/cdaac/doc/documents/Sokolovskiy_newroam.pdf

Development of GNSS-RO Operators for JEDI/UFO

The Joint Effort for Data assimilation Integration (JEDI) is an effort at the Joint Center for Satellite Data Assimilation (JCSDA) to build the next generation unified data assimilation framework for all JCSDA partners and the wider community. This framework will accommodate both operational and research needs through use of the modern software development techniques and tools. One of the important components of JEDI is the Unified Forward observation Operator (UFO). Following the JEDI strategy, the UFO should be model agnostic, modularized, portable and reliable. Such an operator will be easily implemented and ported to a variety of systems and computing platforms, which provides the opportunity to be adopted by operational applications without duplicate development. In addition, when the UFO is coupled with a verification system, it can provide verification against other observation types inside the UFO, including non-traditional observation types (e.g., radiance, radar, radio occultation, etc.).
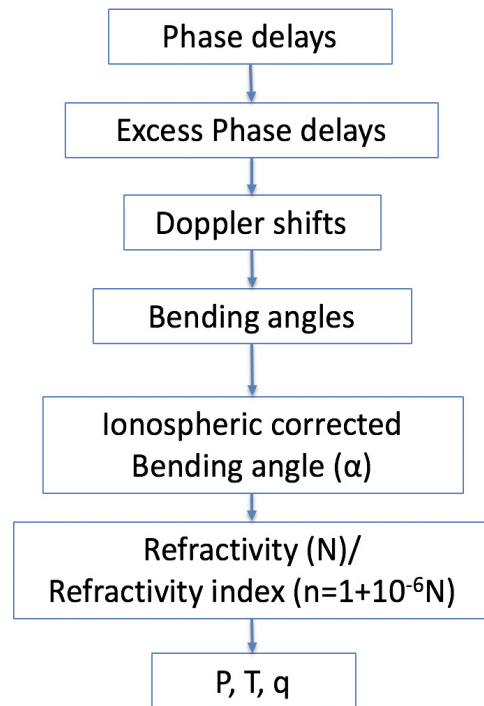
Development of the UFO is essential for the Global Navigation Satellite System Radio Occultation (GNSS-RO) data assimilation effort at the JCSDA. The ultimate goal of this task is to improve and accelerate the use of these measurements in operations. For the past few months, the JCSDA has developed the GNSS-RO UFO based on existing GNSS-RO data assimilation forward operators at multiple operational centers. This paper provides a progress report on this effort, as well as the preliminary results on the validation and comparison of current forward operators for GNSS-RO.

GNSS-RO Measurements and Retrievals

Unlike the other satellite measurements, the GNSS-RO technique relies on optical properties of radio signals, as well as the geometry relationship with respect to Earth, signal transmitters (i.e., GNSS satellites), and receivers (Low Earth Orbit (LEO) satellites, balloons, airplanes, etc.). *Figure 1* shows a schematic flowchart of the GNSS-RO measurements and retrievals. Briefly, it starts with "raw" measurements of the phase delay of radio signals received at two microwave frequencies during an occultation. An occultation occurs when one object (e.g., a GNSS satellite) is hidden by another object (e.g., Earth) that passes between the first object and the observer (e.g., the RO receiver on board a LEO satellite). Following the calibration and correction procedures for instrument errors, path and time delays, and ionospheric effects, the GNSS-RO technique provides measurements of the bending angle, a quantity to describe the bending of the specific ray path due to the atmospheric refraction. Further assuming local spherical symmetry, where the impact parameter is a constant and the refractivity index is only a function of the radial distance (r) of the ray path to

Figure 1. Schematic flowchart of GNSS-RO measurements and retrievals.

Phase delays

Excess Phase delays

Doppler shifts

Bending angles

Ionospheric corrected Bending angle (α)

Refractivity (N)/ Refractivity index (n=1+10⁻⁶N)

P, T, q

the local curvature center, the atmospheric refractivity index (n) can be derived via the Abel inversion integral (Fjeldbo and Eshelman, 1968; Fjeldbo et al., 1971) as:

(1)
$$n(r) = exp \left(\frac{1}{\pi}\int_a^\infty \frac{\alpha(x)}{\sqrt{x^2-a^2}}dx\right)$$

For completeness, the "forward" Abel integral is given as:

(2)
$$\alpha(a) = -2a \int_a^\infty \frac{\frac{dlnn(x)}{dx}}{\sqrt{x^2-a^2}} dx$$

where α is the bending angle, a is the impact parameter, and $a = nr$, r is the radius of the ray path from the local curvature center.

The atmospheric refractivity (N) is:

(3)
$$N = (n-1) \times 10^6$$

Note the Abel transform can only be performed when the impact parameter (a) above the receiver location is known, which is the case for the receivers on board a LEO satellite. However, for receivers inside atmosphere (e.g., balloons, airplanes), the ray path of the GNSS-RO signals does not go through the whole atmosphere and then other approaches might be necessary to achieve the numerical inversion for refractivity (e.g., a ray-tracing method). The following sections focus on GNSS-RO observations using LEO receivers.

The atmospheric refractivity is associated with geophysical quantities via (Bean and Dutton, 1968; Hajj et al., 2002):

(4)
$$N = a_1\frac{p}{T} + a_2\frac{p_w}{T^2} + a_e\frac{n_e}{f^2} + a_wW_w + a_iW_i + O(f^{-3})$$

where $p_w = \dfrac{p}{0.622+0.378q}$ is the water vapor partial pressure, p is the air pressure, T is the temperature, q is the specific humidity, n_e is the electron density, W_w and W_i are the liquid water and ice contents, f is the operating frequency, and $a1$, $a2$, a_e, a_w, and a_i are constant coefficients for each term, respectively.

For neutral atmosphere, the electron density term can be neglected after the ionospheric correction process. The contribution of water and ice are considerably small compared with other terms in the equation and can be therefore neglected as well (Kursinski et al., 1997; Solheim et al., 1999). Then, the atmospheric refractivity (N) is simply a function of T, p, and q:

(5)

$$N = a_1 \frac{p}{T} + a_2 \frac{p_w}{T^2} = a_1 \frac{p}{T} + a_2 \frac{p}{T^2(0.622+0.378q)}$$

Given a prior information of one of these three state variables (e.g., climatology of T), the other two variables can be then derived using Equation (4), together with the equation of state and the hydrostatic equilibrium equation.

Figure 2. Methodology and relationship of various GNSS-RO forward operators.
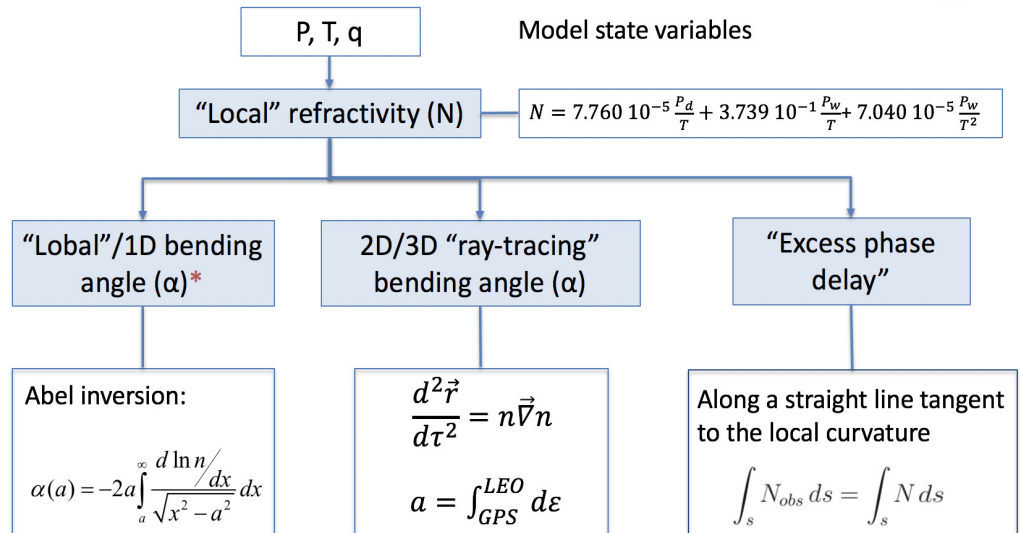
* indicates this Abel inversion method is only applied to GNSS-RO data obtained through LEO receivers

Methodology of GNSS-RO Forward Operators

Given the work flow in *Figure 1*, a GNSS-RO forward operator is generally framed as a bottom-up problem, simulating a selected GNSS-RO observed quantity starting from the model state variables, T, p, and q, at observation locations. Selection of the observational quantity is always a trade-off. The "rawer" the observation quantity is, the less error introduced through the retrieval process, but the more complex and computationally expensive the forward operator would be. At present, most of the operational systems prefer to use either bending angle or refractivity for data assimilation.

The methodology and relationship of alternative GNSS-RO forward operators are depicted in *Figure 2* and briefly described as follows:

Refractivity. A simply way to assimilate refractivity is to take Equation (5) or its variant as the forward operator to compute the atmospheric refractivity from the model state (T, p, and q). This is a common approach taken by many data assimilation systems, e.g., the Gridpoint Statistical Interpolation (GSI) system and the Weather Research and Forecast model Data Assimilation (WRFDA) system. However, it simulates the refractivity pertaining to the tangent point, while the observed refractivity is related to integrated information along the specific ray-path. Alternatively, another way to compute refractivity is to first simulate bending angle (e.g., via a ray-tracing method) and then use the Abel inversion to achieve refractivity following the observation retrieval procedure *(Figure 1)*. However, this approach does not show much more benefits than assimilating bending angle directly and, therefore, is not widely used.

Bending angle. Compared with refractivity, GNSS-RO bending angle is relatively simpler in terms of its retrieval process and observation error characteristics. Assimilation of bending angle is currently adopted by many operational centers, e.g., the National Oceanic and Atmospheric Administration (NOAA), the National Centers for Environmental Prediction (NCEP), the Fleet Numerical Meteorology and Oceanography Center (FNMOC), and the European Centre for Medium-Range Weather Forecasts (ECMWF).

One approach for the bending angle operator is to compute bending angle via Equation (2) from refractivity (computed via Equation (5) a prior). This approach assumes local spherical symmetry. In practice, the integration in Equation (2) requires one vertical profile of the model state (T, p, and q) at each tangent point; therefore, this approach is often denoted as the "local" or 1D bending angle operator. The JCSDA implemented this approach in the GSI system (Cucurull et al., 2007; Cucurull, 2010). NCEP and the National Aeronautics and Space Administration (NASA) are using this approach for their operations. The Radio Occultation Meteorology Satellite Application Facilities (ROM-SAF), managed by the European Organization for the Exploitation of Meteorological Satellites (EUMETSAT), has built a Radio Occultation Processing Package (ROPP). This package also contains such an operator (Healy and Thépaut, 2006), which was adopted by the U. S. Naval Research Laboratory (NRL) and delivered to their operational partner FNMOC for operational data assimilation.

A more accurate, yet more complex, approach for bending angle assimilation is to simulate bending angle via a ray-tracing method. It solves a ray-trajectory equation, which governs the behavior of the radio signal wave under the influence of a refractivity field. The bending angle can be computed by following the ray path. When expressed in a Cartesian coordinate, the equation is written as (Kravtsov and Orlov, 1990):

(6)

$$\frac{d^2\mathbf{r}}{ds^2} = n\nabla n$$

where r is the position vector pointing from the Earth's center to the ray trajectory in the Cartesian coordinate, s is defined by $ds = \frac{dl}{n}$, where l is the length of the ray path and ds is the differential displacement along the ray path. A commonly used form of the ray equation is a set of first-order differential equations:

$$\frac{d\mathbf{r}}{ds} = \mathbf{t}$$

$$\frac{d\mathbf{t}}{ds} = n\nabla n$$

In polar coordinates, these equations can be written as:

$$\frac{dr}{ds} = cos\phi$$

$$\frac{d\theta}{ds} = \frac{sin\phi}{r}$$

$$\frac{d(\theta + \phi)}{ds} = -\frac{sin\phi}{n}\left(\frac{\partial n}{\partial r}\right)_\theta + \frac{cos\phi}{nr}\left(\frac{\partial n}{\partial \theta}\right)_r$$

where r and θ are the radius and the polar angle at an arbitrary point on the ray path, respectively, ϕ is the local zenith angle of the ray path.

The ray-trajectory equation can be numerically solved for any given 3D field of n, once either initial conditions (initial position and direction) or boundary conditions (two end point positions) of the ray are prescribed. The boundary problem may require a ray-shooting method (expensive) and is subject to multiple solutions due to multi-path propagations (Zou et al., 1999). Therefore, it is typically solved as an initial value problem. For the past 20 years, variants of bending angle ray-tracing operators have been proposed (e.g., Hoeg et al., 1995; Zou, et al., 2002; Healy et al., 2007; Wee, et al., 2010).

The ray-tracing method can be simplified by solving the equation in multiple 2D "occultation planes," defined geometrically by the positions of the GNSS and LEO satellites and the local curvature center. Such a bending angle operator is often denoted as a 2D bending angle operator. Implementation of a 2D bending angle operator is more challenging than the other 1D operators, since it requires multiple slices of the model state along the specific ray path for one point bending angle computation. For operational implementation, it is critical to develop an efficient parallel computing scheme (Healy, 2014). Currently, the EUMETSAT ROPP 2D bending angle operator (Healy, et al., 2007; Healy, 2014) is adopted by the operational data assimilation system at ECMWF.

Intermediate approaches. The ray-tracing method accounts for the observed integrated effects along the ray-path. However, it is computationally more expensive than the 1D refractivity and bending angle operators. Multiple efforts were made for intermediate approaches (e.g., Syndergaard et al., 2005; Sokolovskiy et al., 2005; Shao et al., 2009). The basic idea of these approaches is to approximate the ray path with a straight line tangent to the ray-path at the tangent point. Since such an approximation is only valid within a certain distance away from the tangent point, these approaches

require additional handling of refractivity by integrating both observed and simulated refractivities along the same straight line. An example of such a data assimilation system is WRFDA and the integrated quantity is denoted as "excess phase" (Chen et al., 2009) or "excess phase delay." This method is computationally cheaper but less accurate than the ray-tracing method due to the additional assumptions and observation handling.

UFO Implementation and Preliminary Results

Building a UFO for GNSS-RO is the first step to advance the GNSS-RO data assimilation at the JCSDA. Unlike the traditional forward operator setup, the JEDI/UFO introduces a standard interface between the model and observation spaces *(Figure 3)*. Following the general UFO framework in JEDI, the interpolation of state variables from the model grids to the observation locations has been divided into two parts: in horizontal and vertical directions. The horizontal part is handled in the model space, while the UFO block handles vertical interpolation, as well as transform of the model state to the

selected observation quantity at observation locations. Interchange of such information between the two blocks are handled by the interface as shown in *Figure 3*, so that the UFO stays model agnostic. The JEDI/UFO framework provides a chance to compare different operators with the same background (model states), observations, as well as any additional handling.

In the latter half of 2018, in collaboration with original developers, the JCSDA has implemented four GNSS-RO operators for JEDI/UFO, based on existing data assimilation systems and packages, including the one-dimensional (1D) refractivity (following GSI implementation), 1D bending angle (following GSI implementation, NCEP operational capability, denoted as bndGSI), 1D ROPP bending angle (NRL/FNMOC capability, denoted as bndROPP1D), and 2D ROPP bending angle (ECMWF operational capability) operators. For 1D operators, only one vertical profile is required for each observation point. For 2D operators, multiple vertical profiles are required along the ray path (Healy, 2014). Presently, the JEDI system is still under development to

*Figure 3. JEDI interface between model state and forward observation operators.*
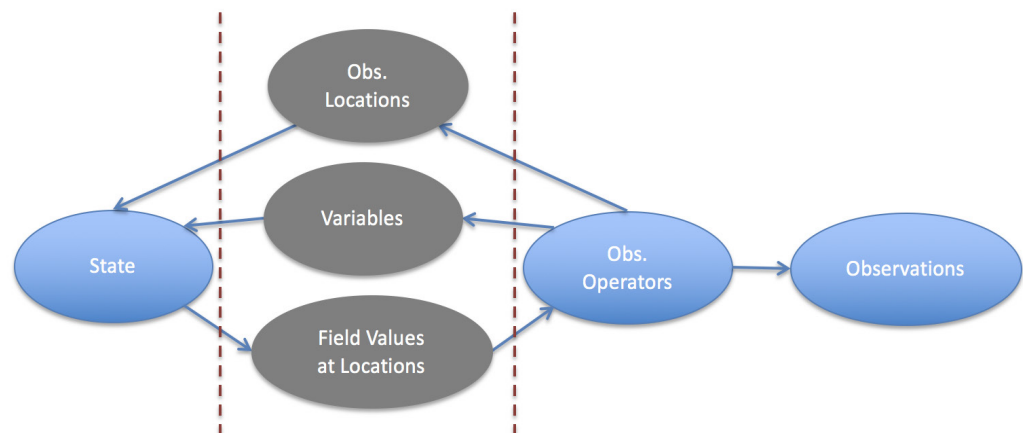
handle the passing of 2D profiles to UFO blocks. Therefore, the following comparison of the operators focus on 1D operators, particularly the 1D bending angle operators.

Figure 4 shows one of the bending angle profiles computed using the two bending angle operators: bndGSI and bndROPP1D. The bending angle values are quite consistent and reasonable for both operators, giving confidence that these two operators are implemented correctly inside JEDI. *Figure 5* shows the normalized biases, the differences between the simulated and observed bending angles (also called "innovation" in a data assimilation system) normalized by the corresponding observed values. The GNSS-RO observations are from NCEP GSI operational data sets within a ±3 hour window centered at 00Z 15 April, 2018. There is a total of 54,943 bending angle measurements at altitudes

up to 50 km. The model state (background) is obtained from the latest NOAA global forecast system on a Finite Volume Cubed-Sphere dynamical core (FV3). Compared with the corresponding observations, the simulations from two operators present similar biases, with larger values at altitudes around and below 10 km and above 40 km. For upper levels, the biases may result from the extrapolation of refractivity beyond model top. For the lower levels, especially below 5 km, radio signals are more ambiguous for many reasons. These include superfraction and ducting situations, and lower-boundary complexity which violates the assumption of local spherical symmetry. Note a data assimilation system always has a quality control procedure based on bias (innovation) values posterior to forward operator computation. Therefore, current operational systems are not likely affected by those outliers with biases larger than

Figure 4. Profiles of bending angle simulated via bndGSI and bndROPP1D.
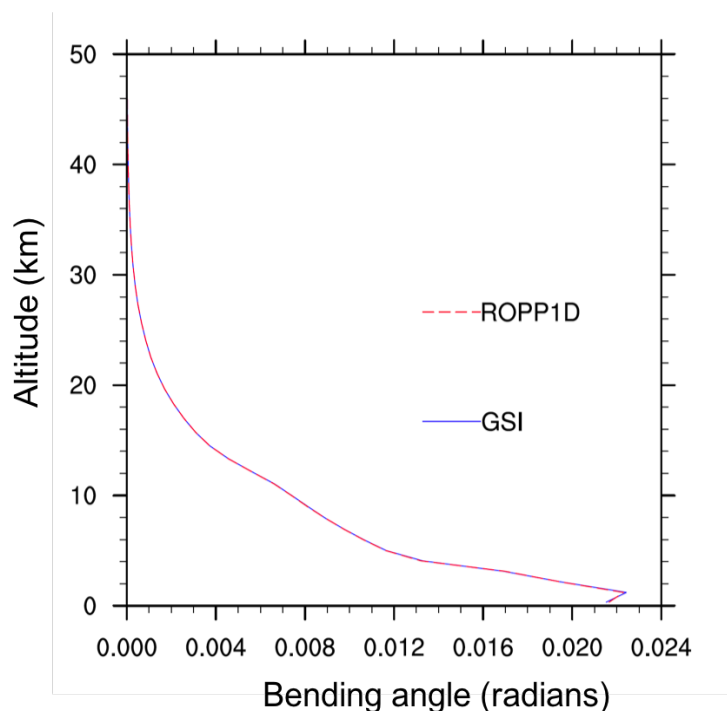
Figure 5. The percentage differences between the simulated and observed bending angles. The differences are normalized by the corresponding observed bending angle. Orange dots mark the results for bndROPP1D and blue dots are for bndGSI.
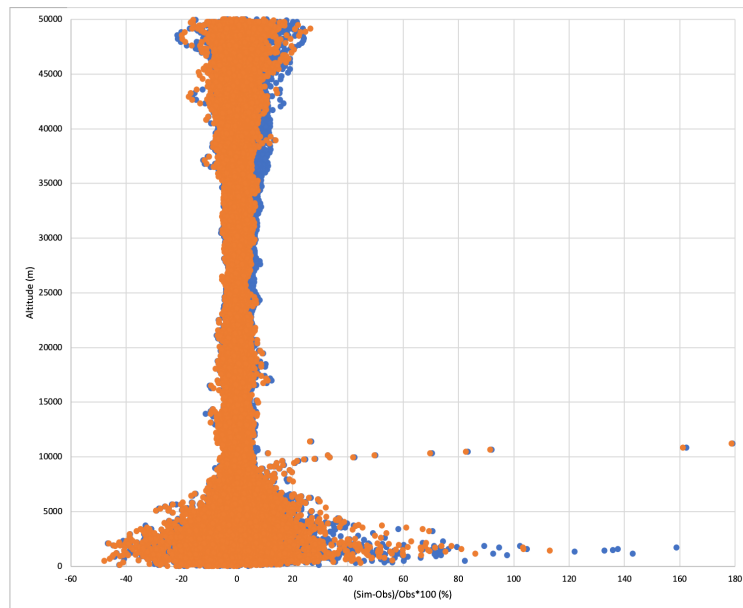
certain threshold values. But this also means fewer observations are being used in those areas. The JCSDA is performing more diagnostics on the results, in order to further improve the performance of these forward operators and, therefore, data assimilation for GNSS-RO.

Following the same methodology, bndGSI and bndROPP2D are implemented differently with respect to numerical solutions and practical considerations. For vertical interpolation, bndGSI uses polynomial interpolation, while bndROPP1D uses bi-linear interpolation (currently other interpolation methods are being investigated at ECMWF). Other differences in these operators include the handling of super-refraction and inclusion of in-line quality control procedures. *Figure 6* shows the scatter plot for the simulated bending angles versus corresponding observations. The x-axis is for observed values while the y-axis is for simulated values. As shown already in *Figure 5*, the

bigger the bending angle values are, the more deviant the simulated bending angles are from observations. While the two operators generate quite consistent results, bndGSI contains more positive outliers, whereas bndROPP1D contains more negative outliers. Two of these outlying profiles are shown in *Figure 7*. Here both operators generate a zig-zag pattern for the low-level bending angle simulation. It may result from various issues, like ducting situation in the background not being removed, a discontinuity in the model states and their gradients due to the vertical interpolation, or the assumption of local spherical symmetry being violated. Closer examination is under way at the JCSDA to identify exact reasons for such misperformances.

Summary and Future Work

In the past few months, the JCSDA has implemented four forward operators for GNSS-RO observations in the framework of JEDI/UFO, based on existing operational capabilities in the United States and at

Figure 6. *Comparison of simulated (y-axis) and observed (x-axis) bending angles. Orange dots mark the simulated results from bndROPP1D and blue dots are for bndGSI.*
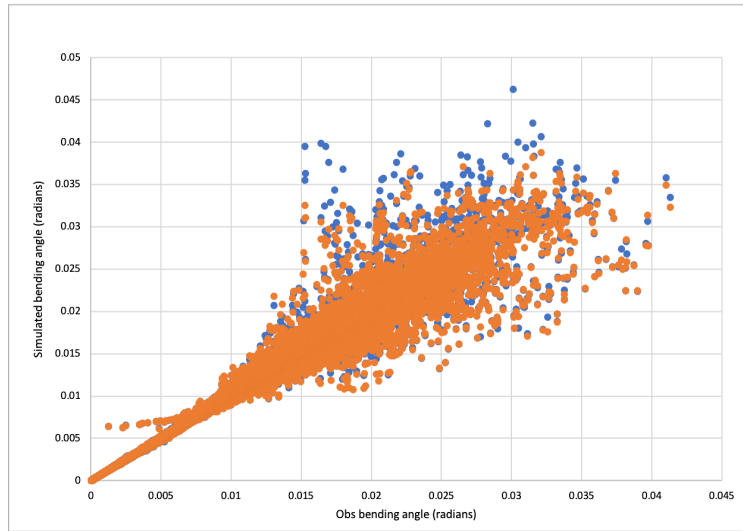
Figure 7. *Profiles of simulated and observed bending angles at two locations with large biases at low levels. Red curves are for profiles from bndGSI, green curves are for bndROPP1D, and black curves are for observed values.*
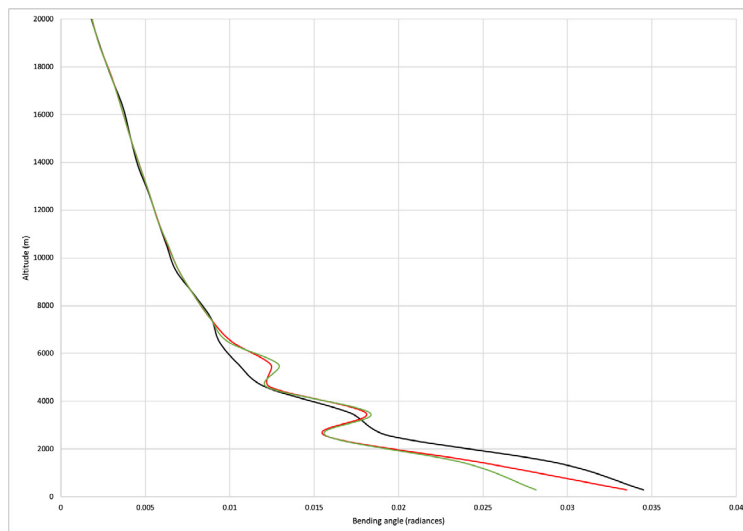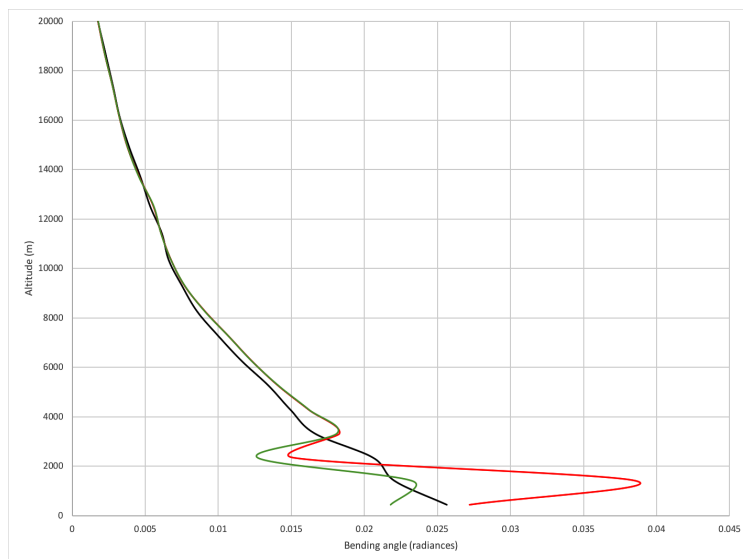
ECMWF. The initial testing and evaluations show all the operators are working reasonably, whereas large biases are found for both operators at altitudes above 40 km and at and below 10 km. Comparing the two 1D bending angle operators provides an insight on the implementation details for the operators. Currently, the JCSDA is performing more diagnostics on the results, with a goal to improve the performance of these operators in the problematic areas. The JCSDA will also perform data assimilation and forecast experiments and further evaluate and optimize the GNSS-RO operators through the impact studies and prepare for the operational to research (R2O) transitions in the future.

It is also noted that the forward operators discussed in this article are based on GNSS-RO observations received from LEO satellites. For receivers inside atmosphere, additional considerations and assumptions may be necessary for their forward operators. Further studies and development will be taken at the JCSDA for other GNSS-RO operators, GNSS-RO observations using other types of receivers, as well as other types of GNSS observations (e.g., precipitable water, reflectometry).

Authors

Hui Shao (JCSDA), François Vandenberghe (JCSDA), Hailing Zhang (COSMIC & JCSDA), Benjamin Ruston (NRL), Sean Healy (ECMWF), Lidia Cucurull (NOAA/OAR).

Reference

Bean, B. R. and E. J. Dutton. Radio Meteorology. Dover Publications Inc., New York, 1968

Chen, S.-Y., C.-Y. Huang, Y.-H. Kuo, Y.-R. Guo, and S. Sokolovskiy, Assimilation of GPS refractivity from FORMOSAT-3/COSMIC using a nonlocal operator with WRF 3DVAR and its impact on the prediction of a typhoon event. Terr. Atmos. Oceanic Sci., 20, 133–154, 2009. doi:https://doi.org/10.3319/TAO.2007.11.29.01(F3C)

Cucurull, L., J.C. Derber, R. Treadon, and R. J. Purser, Assimilation of global positioning system radio occultation observation into NCEP's Global Data Assimilation Assimilation System. Mon. Weather Rev., 135, 3174-3193, 2007

Cucurull L., Improvement in the use of an operational constellation of GPS radio occultation receivers in weather forecasting. Wea. Forecasting, 25, 749-767, 2010

Fjeldbo, G. and V. R.Eshlemann. The atmosphere of Mars analyzed by integral inversion of the Mariner IV occultation data. Planet Space Sci., pages 1035–1059, 1968

Fjeldbo, G. and A. J. Kliore. The neutral atmosphere of Venus as studied with the Mariner V radio occultation experiments. Astron. J., pages 123–139, 1971

Hajj, G. A. and et al. A technical description of atmospheric sounding by GPS occultation. Journal of Atmospheric and Solar-Terrestrial Physics, 64:451–469, 2002

Healy, S. B. and J. -N. Thépaut, Assimilation experiments with CHAMP GPS radio ocuultation measurements. Quart. J. Roy. Meteorol. Soc., 132, 605-623, 2006

Healy, S. B., J. R. Eyre, M. Hamrud, and J-N. Thepaut. Assimilating GPS radio occultation measurements with two-dimensional bending angle observation operators. Quart. J. Roy. Meteor. Soc., 133, 1213–1227, 2007

Healy, S., Implementation of the ROPP two-dimensional bending angle observation operator in an NWP system, ROM SAF Report 19, 2014

Hoeg, P., A. Hauchecorne, G. Kirchengast, S. Syndergaard, B. Belloul, R. Leitinger, and W. Rothleitner. Deviation of the atmospheric properties using radio occultation technique. Technical Report Scientific Rep. 95-4, Danish Meteorological Institute, 1995

Kravtsov, Y. A. and Y. I. Orlov. Geometrical Optics of Inhomogeneous Media. Springer-Verlag, New York, 1990

Kursinski, E. R. and et al. Observing earth's atmosphere with radio occultation measurements using the global positioning system. J. Geoph. Res., 102:23,429–23,465, 1997

Shao, H., X. Zou, and G. A. Hajj. Test of a non-local excess phase delay operator for GPS radio occultation data assimilation. J. Appl. Remote Sens.,3, 033508, 2009

Sokolovskiy, S., Y-H. Kuo, and W. Wang. Assessing the accuracy

of a linearized observation operator for assimilation of radio occultation data: Case simulations with a high-resolution weather model. Mon. Wea. Rev., 133, 2200–2212, 2005

Solheim, F. S., J. Vivekanandan, R. H. Ware, and C. Rocken, 1999: Propagation delays induced in GPS signals by dry air, water vapor, hydrometeors, and other particulates. Journal of Geophysical Research-Atmospheres, 104, 9663-9670, doi:10.1029/1999JD900095

Syndergaard, S., E. Kursinski, B. Herman, E. Lane, and D. Flittner. A refractive index operator for assimilation of occultation data. Mon. Wea. Rev., 133, 2650–2668, 2005

Wee, T.-K., Kuo, Y.-H., and Lee, D.-K.: Development of a curved ray tracing method for modeling of phase paths from GPS radio occultation: a two-dimensional study, J. Geophys. Res., 115, D24119, doi:10.1029/2010JD014419, 2010

Zou, X., H. Liu, and R. A. Anthes. A statistical estimate of errors in the calculation of radio-occultation bending angles caused by a 2d approximation of ray tracing and the assumption of spherical symmetry of the atmosphere. Journal of Atmospheric and Oceanic Technology, 19:51–64, January 2002

Zou, X., F. Vandenberghe, B. Wang, M. E. Gorbunov, Y.-H. Kuo, S. Sokolovskiy, J. C. Chang, J. G. Sela, and R. A. Anthes. A raytracing operator and its adjoint for the use of gps/met refraction angle measurements. J. Geophy. Res., 104:22,301–22,318, 1999

# Assessment of Radio-Occultation from Multiple GNSS Platforms: Operational & Non-Operational

There is an on-going effort at Joint Center for Satellite Data Assimilation (JCSDA) to provide an assessment of the existing operational Global Navigation Satellite System – Radio Occultation (GNSS-RO) observations from multiple platforms. The radio-occultation (RO) platforms currently operational and available at National Centers for Environmental Prediction (NCEP) are COSMIC-1, METOP-A, METOP-B, TanDEM-X, and TerraSAR-X. This article also includes evaluation of two new RO sensors on-board the platforms of Korea Multi-Purpose Satellite-5 (KOMPSAT-5) and PAZ (formerly known as SEOSAR/ PAZ - Satélite Español de Observación Synthetic Aperture Radar). Onboard KOMPSAT-5 is a space-borne integrated dual-frequency GPS occultation receiver (known as Integrated GPS Occultation Receiver (IGOR)) responsible for capturing the RO measurements. PAZ carries the advanced GPS receiver IGOR+, which captures the polarimetric radio occultation observations. KOMPSAT-5 and PAZ-RO data was obtained from COSMIC Data Analysis and Archive Center (CDAAC), UCAR.

The present report describes the preliminary phase of the work towards assessment and evaluation of GNSS-RO platforms. This is intended towards investigation of the model response to the observation and, in-addition, the data quality is evaluated. Currently operational GNSS-RO observations, including the two non-operational platforms, are used for calculation of the 'Observation (O) – Background (B)' (OmB) statistics. NCEP's presently operational 4D-EnVar Gridpoint Statistical Interpolation (GSI) analysis system is used as the assimilation code. The background information or the first guess (as is commonly known) are accepted from the 6-hour forecast from NCEP's operational suite. The results discussed here can be categorized as pre-minimization diagnostics. The GNSS-RO platforms included in the diagnostics are MetOp-A and MetOp-B (MetOp), TERRA (terra), TANDEM (tandm), PAZ (pazro), COSMIC-1 (cosm1), and KOMPSAT-5 (komp5). Only the setting profiles of komp5 have been used for the assessment. The time period for this work is 11th May – 9th June, 2018. A GNSS-RO Evaluation and Monitoring toolkit was developed at JCSDA for the preliminary assessment and monitoring of the GNSS-RO platforms. The first version of the toolkit has been released to the community and is used for the present study.

Figure-1 shows the total number of daily occultation profiles for the study period. Some days of data gap is observed for both tandm and terra; metop, which includes both MetOp - A and B, has the highest number of daily occultation profiles as compared to other platforms. tandm has the least number of profiles. Use of only setting occultation for

Figure 1. *Daily number of occultation profiles for the period 11th May – 09th June, 2018.*
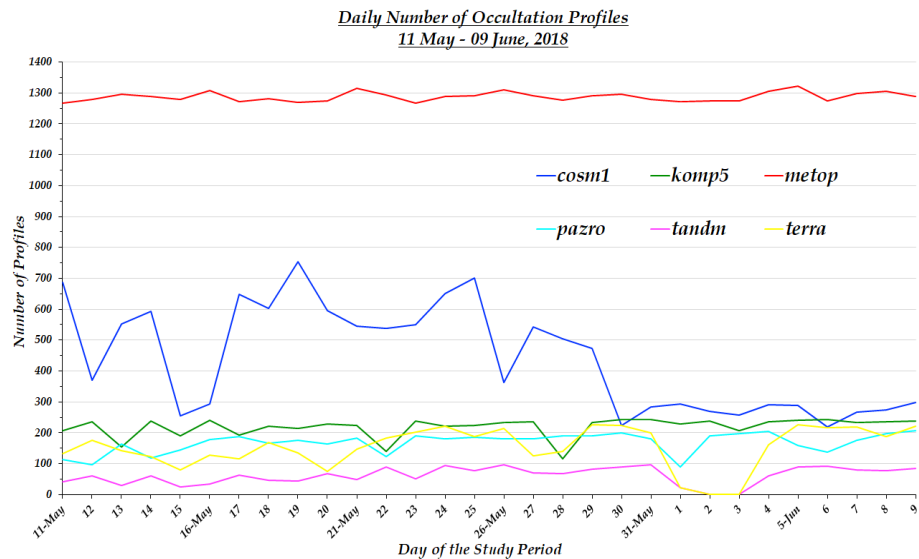
komp5 has lowered its daily number of profiles available to the assimilation system. The profile numbers for cosm1 are unstable and vary in large numbers throughout the study period. Occultation profiles for pazro is lower than komp5 but is stable for this period. *Figure-2* gives the mean observation count with respect to the pressure levels (hPa) at pre-minimization state.

These are the mean count of RO data that are available for assimilation into the GSI system. The values are likely to change during the minimization procedure, which results in reduction in the number of RO observations getting assimilated. The vertical distribution pattern through the pressure levels remains the same for all the platforms. The observation count increases with height and is maximum beyond the 50hPa pressure level. metop has the highest and tandm the lowest observation count. The accepted observations from metop are available from the level of 650hPa onwards. The vertical distribution of observation count is similar for komp5, pazro, and terra.

*Figure 2.* *Mean Observation Count with respect to pressure (hPa) levels for the period 11th May – 09th June, 2018.*
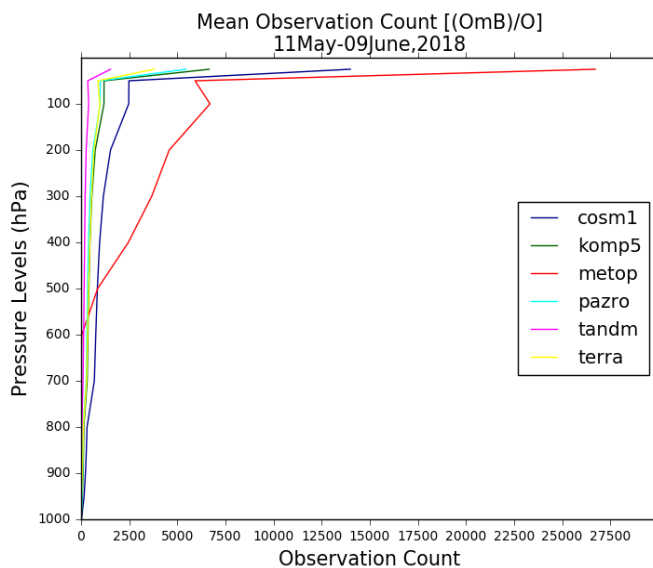
Bias and Root Mean Square (RMS) of (O-B) are two important parameters required to assess the data quality as a response of the weather model towards the observation set. *Figures 3* and *4* depict the vertical profile of the mean bias (in %) and RMS of (O-B), respectively; each quantity being represented as values normalized with the observation (O). Tandm is seen to have high negative bias close to the surface as compared to other platforms and has higher positive bias at 850hPa *(Figure 3)*. Similar to tandm, but lower in magnitude, cosm1 has higher positive bias at 850hPa and negative bias close to the surface. *Figure 4* supplements the information obtained from *Figure 3*. From around 600-300hPa metop has lower RMS of [(O-B)/O] compared to

Figure 3. Mean Bias [(OmB)/O] (%) with respect to pressure levels for the period 11th May – 09th June, 2018.

Mean Bias[(OmB)/O]
11May-09June,2018
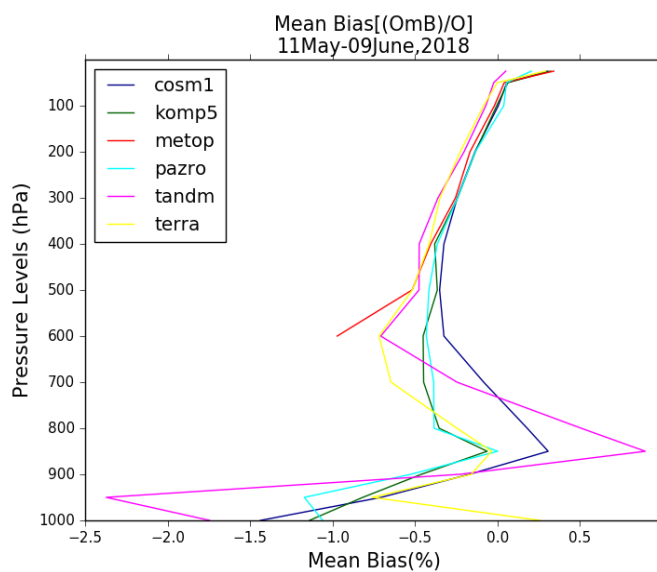
Figure 4. Mean RMS of [(OmB)/O] with respect to pressure levels for the period 11th May – 09th June, 2018.

RMS [(OmB)/O]
11May-09June,2018
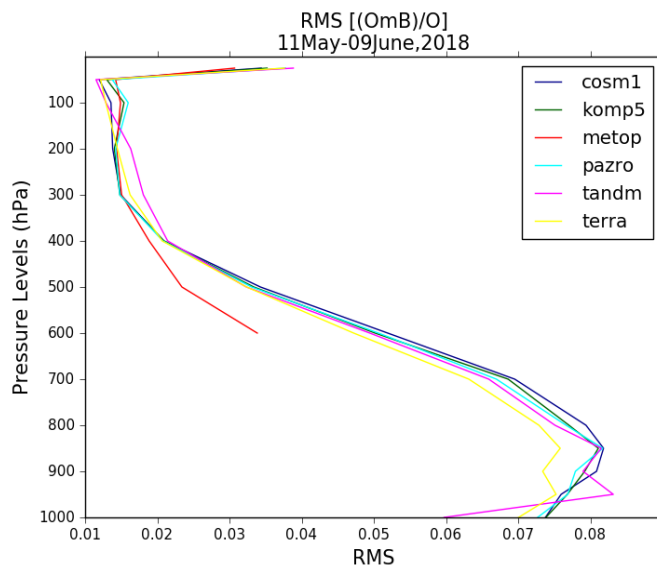
other platforms. The quantitative estimate of both mean bias and RMS of [(O-B)/O] for all the other platforms have minor differences close to the surface but are comparable over higher altitudes. The vertical profiles of pazro and komp5 have close estimate for both the statistics.

A certain percentage of observations are rejected from the entire dataset each time due to the application of quality control procedures. Vertical profile of these rejection percentages are depicted in *Figure 5*. The highest percentage of data are rejected from the pressure level of 50 – 0hPa, for each of the platforms. Over lower to middle atmosphere, rejection percentage for metop is highest but metop is lowest over the higher levels.

There are typically four rejection criteria imposed during the quality control. They are: (1) Observations are outside the vertical boundary of the sigma levels; (2) Observations are at height above 50 km above the ground; (3) the ratio (Innovation Vector/Obs. Error) > Gross Error Parameter; (4) Observations are close to or inside the model super refractivity layer. *Figure 6* represents the percentage of rejection due to each criterion described above. All metop observations below 8 km are rejected due to the large discrepancies when compared against the NCEP model background (depicted as criteria 4 in *Figure 6*). For the other platforms, the percentage of rejection is largest due to criterion 1, for them being outside the vertical boundary of the sigma levels. Rejection due to criterion 2 is the lowest.

Results from this preliminary assessment of PAZ GNSS-RO data shows that its quality is very similar to that of KOMPSAT-5 RO observations. This is encouraging because, earlier, JCSDA conducted a comprehensive evaluation of KOMPSAT-5 products and recommended the data for operations. This new evaluation also shows a degradation in

Figure 5. Percentage of Data Rejected with respect to pressure levels for the period 11th May – 09th June, 2018.
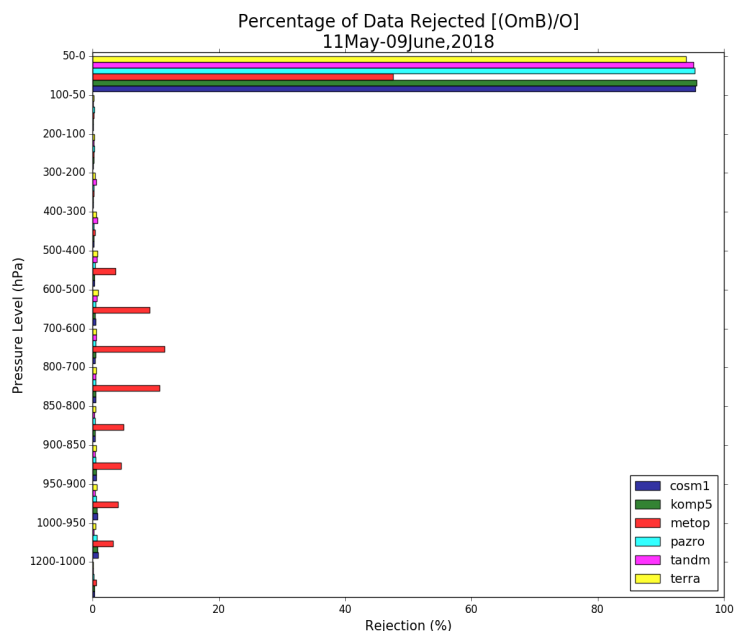
Figure 6. Percentage of Data Rejected due to the Rejection Criteria of Quality Control for the period 11th May – 09th June, 2018.

Percentage of Data Rejected [(OmB)/O]
11May-09June,2018
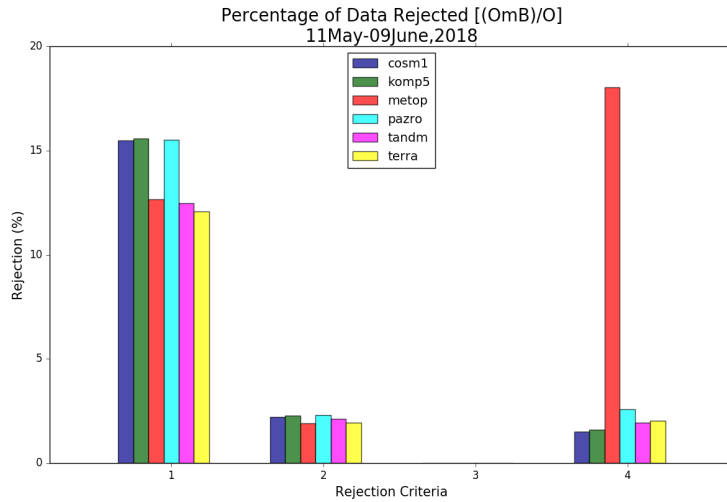
COSMIC-1 data quality compared to earlier studies made with the observation from this same platform. This degradation is caused by the aging satellites. The COSMIC constellation was launched in 2006 with a nominal mission of 3 years. Overall, the quality of observations from PAZ is found to be similar to the current operationally assimilated RO datasets: METOP, TANDM and TERRA. Additional evaluations are in the process at JCSDA to confirm these preliminary results and a recommendation whether to use PAZ observations for operations will be made.

Authors

Suryakanti Dutta (JCSDA), François Vandenberghe (JCSDA), Hui Shao (JCSDA), Hailing Zhang (COSMIC & JCSDA), and James Yoe (JCSDA).

Error Characteristics of KOMPSAT-5 Radio Occultation Observations

The global navigation satellite system (GNSS-RO) radio occultations (RO) from many missions have been assimilated into numerical weather prediction (NWP) in the major operational centers around the globe (e.g., Healy and Thépaut 2006; Cucurull et al., 2007; Poli et al., 2008) and have been proven valuable. The Korea Multi-Purpose Satellite-5 (KOMPSAT-5; 2013) RO data are recently available in real-time, and efforts are ongoing to make them assimilated operationally (Dutta et al., 2018). As observation error (OE) specification is vital in data assimilation (DA); this study demonstrates the OE characteristics of KOMPSAT-5 RO bending angles by comparing five OE estimations that are named as SOE, DyOE, EnOE, DdOE, and DdOE_dy, respectively in this article. The NCEP operational Gridpoint Statistical Interpolation (GSI; Wu et al., 2002, Kleist et al., 2009) specifies the bending angle OEs by pre-defined statistical-based functions (Cucurull 2010), and we refer to it as static OE (SOE). A proxy of OE estimate for each individual observation based on the local spectral width (LSW) is provided for the COSMIC and KOMPSAT-5 bending angles in the latest data processing of COSMIC Data Analysis and Archive Center (CDAAC). Originally introduced by Gorbunov et al. (2006), LSW is closely associated to refractivity irregularities present in the moist low troposphere (Sokolovskiy 2014). A dynamic OE estimate (DyOE) profile can be derived for each occultation based on its LSW. By definition, DyOEs provide a dynamical error estimate for each individual bending angle. Following Kuo et al. (2004) and Chen et al. (2011), we estimate the ensemble-based OE value (EnOE) through its association with the apparent error and the background error. The background error is sampled by the ensemble spread of a set of ensemble forecasts. We also have two sets of OEs following Desroziers et al. (2005) that developed a set of consistency diagnostics under the linear estimation theory of DA schemes based on the combinations of observation-minus-analysis (OMA), observation-minus-background (OMB), and analysis-minus-background (AMB). Since DA analysis is involved in this calculation, an initial OE specification is needed. We use SOE and DyOE as initial OEs for the Desroziers OE estimates respectively, and refer the two sets of OE as DdOE, and DdOE_dy. While Desroziers et al. (2005) proposed primarily the consistency diagnostics to estimate OE, they also argued that the diagnosed error covariance can be applied to the subsequent assimilation and thus to iteratively achieve a refinement of the error covariances. We do not apply further iterations/tuning, but instead we compare DdOE and DdOE_dy, along with other estimates. Among the five OE estimations, SOE and DyOE are considered as in observation stage, while EnOE, DdOE, and DdOE_dy are diagnostic-based and thus can be used to evaluate the first two estimates.

We conduct DA experiments with the GSI system on a three-dimensional ensemble-variational hybrid analysis mode (3DEnVar) at a horizontal resolution of T574 over two one-month periods, in August 2016 and January 2018, to represent the Northern Hemispheric summer and winter, respectively. The experiments are carried out in a non-cycling mode, and the backgrounds and ensemble forecasts are from the NCEP Global Data Assimilation System (GDAS) 6 h deterministic global forecasts and ensemble forecasts of 80 members. The operational RO data, along with the conventional in situ observations, cloud-motion vectors, and satellite radiances, are also from the NCEP GDAS archive. KOMPSAT-5 data were obtained from CDAAC. KOMPSAT-5 data are processed in a similar manner as to COSMIC data in terms of quality control procedure and vertical thinning.

Figure 1 displays distributions of the fractional DyOE at 2 km above mean sea level (MSL) for KOMPSAT-5 RO soundings in August 2016 and January 2018, respectively. The DyOEs show large occultation-to-occultation variations with season, region, and underlying terrain type. They are generally larger over tropical regions than in high latitudes, larger over oceans than over lands, and are larger in the summer hemisphere (Northern Hemisphere in August and Southern Hemisphere in

Figure 1. Distribution of KOMPSAT-5 bending angle fractional DyOE at 2 km MSL for (a) August 2016 and (b) 2018.
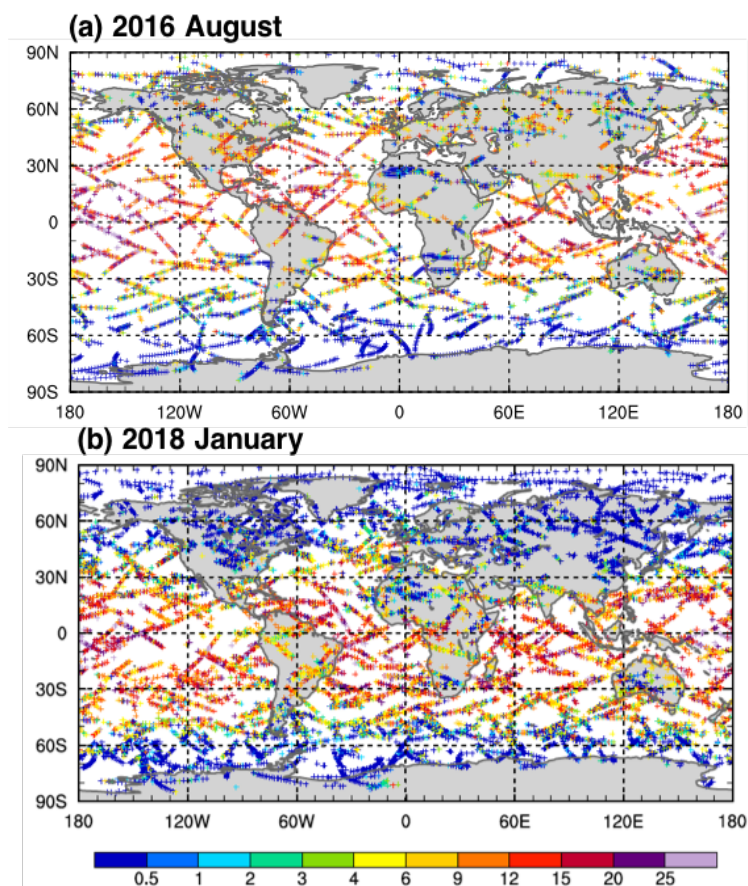
January) than in the winter hemisphere (Southern Hemisphere in August and Northern Hemisphere in January) since DyOEs in the lower troposphere are closely related to the random refractivity irregularities and the variation of water vapor distribution.

RO observations are sorted by horizontal bins of 10°×10° in given layers, and the bin-averaged statistics are compared among the five sets of OEs. The three diagnostic-based estimates, EnOE, DdOE, and DdOE_dy are in good agreement during both experimental periods (not shown), although they are based on different estimation methods. Specifically, EnOE is estimated with OMBs and independent ensemble forecasts, while DdOE and DdOE_dy are based on OMAs and OMBs for different initial OE specifications. *Figure 2* shows scatter plots between each of the three diagnosed EnOE, DdOE, and DdOE_dy estimates and the prescribed SOE and DyOE estimates. DyOE matches all the diagnostic-based estimates with higher correlation coefficients than SOE does. The correlation coefficient between

DyOE and DdOE_dy is 0.902 for DyOE, while it is only 0.66 between DyOE and SOE. It can also be seen that SOEs are separated in two groups, which are related to the binary aspect of its statistical specification with latitude. DyOEs span broadly with extremely small and big values, which are associated with the tropical oceans and the high latitudes. It is not surprising that SOE matches DdOE better than it matches the other two. This is because DdOE is based on the consistency diagnostics that uses the SOE initial specification in DA. Similarly, DyOE best correlates to DdOE_dy, since the latter is based on the diagnostics that uses the former as initial specification.

While OE characteristics of KOMPSAT-5 data (global patterns, bias, vertical distribution, representativeness error, comparison with COSMIC data, etc.) will be presented in detail in a comprehensive report (Zhang et al., 2019; in preparation), this short article briefly demonstrates that the correlation coefficients between DyOE and the three diagnostic-based estimates are consistently higher than that between SOE

Figure 2. Scatter plots showing comparison between each of the three diagnostic-based estimates (EnOE, DdOE, and DdOE_dy) and (a-c) SOE and (d-f) DyOE for KOMPSAT-5 data in August 2016 in the layer of 700–500 hPa. r in each panel represent the correlation coefficient.
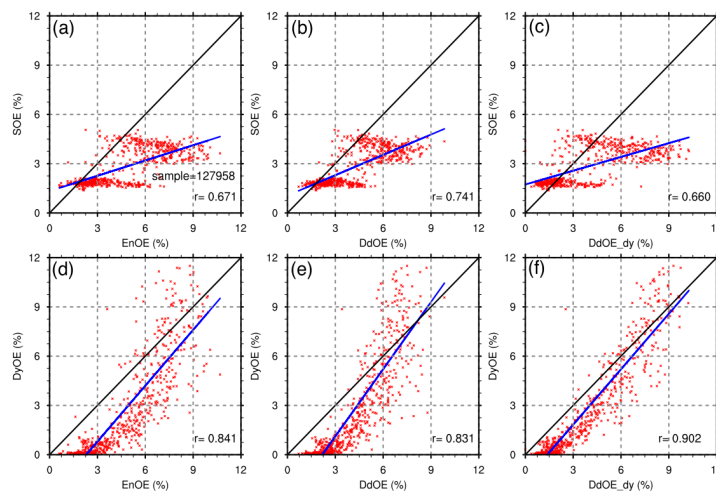
and the diagnostic-based estimates. Work is ongoing to optimally use the dynamic information in DyOEs in data assimilation. We expect the dynamic estimate of bending angle OEs can help improve RO data impact on NWP in a near future.

Authors

Hailing Zhang (COSMIC & JCSDA), François Vandenberghe (JCSDA), Ying-Hwa Kuo (UCAR/UCP) and Tom Auligné (JCSDA).

References

Chen, S.-Y., C.-Y. Huang, Y.-H. Kuo, and S. Sokolovskiy, 2011: Observational Error Estimation of FORMOSAT-3/COSMIC GPS Radio Occultation Data. *Mon. Wea. Rev.*, 139, 853–865.

Cucurull, L., and J. C. Derber, R. Treadon, and R. J. Purser, 2007: Assimilation of Global Positioning System radio occultation observations into NCEP's Global Data Assimilation System. *Mon. Wea. Rev.*, 135, 3174–3193.

Cucurull, L., 2010: Improvement in the use of an operational constellation of GPS radio occultation receivers in weather forecasting. *Wea. Forecasting*, 25, 749–767.

Desroziers, G., L. Berre, B. Chapnik, and P. Poli, 2005: Diagnosis of observation, background and analysis-error statistics in observation space. *Q. J. R. Meteorol. Soc.*, 131, 3385–3396.

Dutta, S., T. Auligne, and J. G. Yoe, Assimilation of KOMPSAT-5 GPSRO in GSI 4D-EnVar assimilation system. 98th AMS annual meeting, 7–11 January 2018, Austin, TX.

Gorbunov, M. E., K. B. Lauritsen, A. Rhodin, M. Tomassini, and L. Kornblueh, 2006: Radio holographic filtering, error estimation, and quality control of radio occultation data. *J. Geophys. Res.*, 111, D10105.

Healy, S. B., and J.-N. Thépaut, 2006: Assimilation experiments with CHAMP GPS radio occultation measurements. *Quart. J. Roy. Meteor. Soc.*, 132, 605–623.

Kleist, D. F. Parrish, J. C. Derber, R. Treadon, R. M. Errico, and R. Yang, 2009: Improving incremental balance in the GSI 3DVar analysis system. *Mon. Wea. Rev.*, 137, 1046–1060.

Kuo, Y.-H., T.-K. Wee, S. Sokolovskiy, C. Rocken, W. Schreiner, D. Hunt, and R. A. Anthes, 2004: Inversion and error estimation of GPS radio occultation data. *J. Meteorol. Soc. Jpn.*, 82, 507–531.

Poli, P., S. B. Healy, F. Rabier, and J. Pailleux, 2008: Preliminary assessment of the scalability of GPS radio occultations impact in numerical weather prediction. *Geophys. Res. Lett.*, 35, L23811.

Sokolovskiy, 2014: Improvements, modifications, and alternative approaches in the processing of GPS RO data. Fifth EUMETSAT ROM SAF Workshop on Application of GPS Radio Occultation Measurements Reading, UK, 16-18 June 2014. Available at https://www.ecmwf.int/en/learning/workshops-and-seminars/past-workshops/fifth-eumetsat-rom-saf-user-workshop-applications-gps-radio-occultation-measurements

Wu, W. S., R. J. Purser, and D. F. Parrish, 2002: Three-dimensional variational analysis with spatially inhomogeneous covariances. *Mon. Wea. Rev.*, 130, 2905–2916.

MEETING REPORT

7th AMS Symposium on the Joint Center for SatelliteData Assimilation

Dr. Yannick Trémolet talks at AMS. Photo credit: Dawn Mullally | CPAESS | UCAR.

The JCSDA held its 7th Symposium at the 99th American Meteorological Society (AMS) Annual Meeting in Phoenix, AZ. The symposium was a full day event on Tuesday, January 8, 2019, with six topical sessions, and one poster session. Presentations and posters were offered by staff and contractors of the JCSDA partner agencies as well as the broad academic community, and by international representatives (e.g., ECMWF, UK Met Office).

Dr. François Vandenberghe presenting his poster at AMS. Photo credit: Dawn Mullally | CPAESS | UCAR.
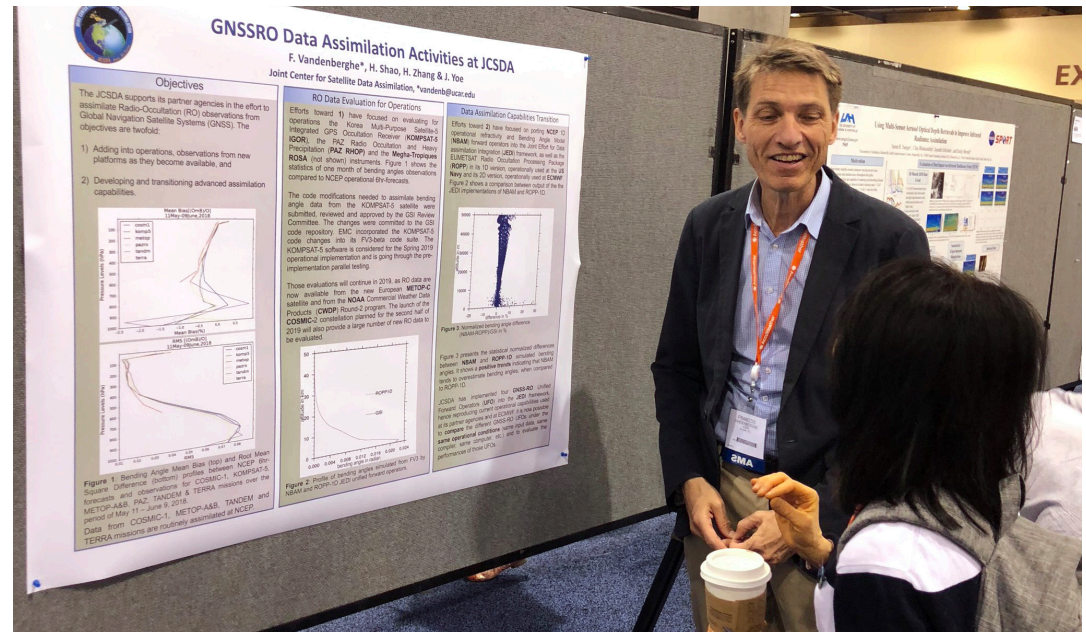
Though the annual meeting was generally affected by the government partial shut-down, the symposium continues to be an important outreach event for the data assimilation community, with strong attendance and stimulating informal discussions on various topics. It also helps boost the communications among JCSDA partners as well as between the JCSDA and external collaborators in the U. S and from international agencies on developing the unified data assimilation capabilities.

The oral sessions featured a total of 18 presentations, dedicated to various aspects of the data assimilation study. The first session was, chaired by Benjamin Johnson (JCSDA), devoted to the New and Improved Data Assimilation Tools and Methods. Followed by the session of Land, Ocean, Cryosphere, Air Quality, and Coupled Earth System Data Assimilation, chaired by Benjamin Ruston (NRL). The third and fourth sessions, chaired by Francois Vandenberghe and Thomas Auligné (JCSDA), were dedicated to the Next-Generation Satellites and Sensors Data Assimilation. Two more oral sessions were held in the afternoon and featured talks on all-sky radiance assimilation, chaired by Hui Shao (JCSDA), and the Joint Efforts for Data Assimilation Integration (JEDI), chaired by Guillaume Vernieres (JCSDA). The JCSDA Symposium also co-sponsored a joint session (invited only), National and International Program Overviews for Environmental satellites, on the morning of Tuesday, January 9.

The Symposium was organized under the leadership of James Yoe (NWS), with contributions from various partners. Unfortunately, a few presenters and chair persons could not make the symposium due to the furlough. However, the support from them as well as those participating the symposium has been and continue to be a great asset of the JCSDA.

Introducing Dr. Hamideh Ebrahimi

Dr. Hamideh Ebrahimi joined NASA's Global Modeling and Assimilation Office (GMAO) in support of the Joint Center for Satellite Data Assimilation (JCSDA) in July, working on the assimilation of surface sensitive microwave radiances and on the implementation of coupled Atmosphere/ocean/sea-ice data assimilation capability within the Joint Effort for Data-assimilation Integration (JEDI) project.

Dr. Ebrahimi earned a PhD in Electrical Engineering with a minor in Planetary Sciences from University of Central Florida, working at the Central Florida Remote Sensing Lab. She has been involved in a number of NASA Earth science satellite mission grants analyzing satellite microwave radiometers data, such as NASA Aquarius, Global Precipitation Measurement (GPM), and the HS3 Hurricane missions. At NASA, she was an active member of the GPM inter-calibration working group. Working there has been very rewarding for her, providing the opportunity to interact with scientists and engineers from NOAA, NASA, and other universities. Through these collaborations, she cooperated with Earth System Science Interdisciplinary Center (ESSIC) at the University of Maryland as a faculty research assistant for seven months during her PhD. Also as part of GPM inter-calibration group, she received a NASA group achievement award in 2015.

After graduation, Hamideh joined the Center for Remote Sensing at the University of Florida as a Postdoctoral Research Associate, working on a variety of projects in applying state-of-the-art Microwave remote sensing and GPS technologies to soil moisture measurements. She was involved in the design, implementation and testing of a Global Navigation Satellite System (GNSS)-Reflectrometry system for measurement of soil properties. In addition to research, she has been involved in mentoring undergrads and college students, has served as a reviewer for Journal of IEEE Transactions on Geoscience and Remote Sensing and Journal of Atmospheric and Oceanic Technology, and has been part of a NASA proposal review panel.

In her leisure time, Hamideh enjoys outdoor activities, such as hiking, biking, camping, and reading about a variety of topics, especially Astronomy and Psychology. She is an active supporter of Child Foundation, which is an international charity organization that helps children living in poverty remain in school.

EDITOR'S NOTE

Greetings - it's exhilarating for me to be back at my desk following a planned absence for the holiday season, followed by a much longer, unplanned one due to the much-publicized lapse in appropriated funding for a number of Federal departments and agencies, which impacted some (though not all) of the JCSDA partners recently. Despite the challenges this situation presented to us individually and corporately, a great deal of work has been accomplished since the last issue of the Newsletter, and we return to our mission with as much zeal and determination as ever.

Although many federal employees of our community were not able to attend the Annual Meeting of the American Meteorological Society in Phoenix, AZ in January, the JCSDA Symposium went forward as planned, providing an excellent opportunity for interaction with our academic, private sector, and international colleagues engaged in developing and testing means to exploit satellite data more effectively in environmental models. Hui Shao of the JCSDA has provided a summary report of the Symposium for this issue. Fortunately the shut-down was concluded in time to hold the annual JCSDA Executive Team Retreat as scheduled February 5-7. The Executive Team and the Project Leads met and completed the preliminary draft of the 2019 Annual Operating Plan.   Currently the plan is being revised and edited, after which it will be reviewed for approval by the Management Oversight Board. Despite the partial shut-down, we remain on schedule to begin execution of the new plan on April 1, 2019.

The proliferation of new and newly-available Global Navigation Satellite System Radio Occultation (GNSS-RO) sensors on orbit presents challenges and opportunities for the JCSDA and the operational users it serves. The work of evaluating these data and improving the means to assimilate them effectively in multiple operational NWP models and DA systems is shared across several of the JCSDA projects, including those for New and Improved Observations, Impact of Observing Systems, and the Joint Environment for Data assimilation Integration. Reviewing and finalizing the Newsletter is always a race against the clock, and this issue proved to be no exception, as I realized there were a solid half-dozen contributions on GNSS-RO to be included, and indeed, this particular issue may look closer to a journal than to a newsletter as a result. Be that as it may, I am confident that you will find a great deal that is new and of value to you in reading these articles.

Finally, we take this opportunity to welcome Dr. Hamideh Eibrahimi, who recently joined the JCSDA. We are pleased to include a short introduction to her work and outside interests among these pages, and we hope that she will find her work here exciting and satisfying.

Jim Yoe

SCIENCE CALENDAR   **UPCOMING EVENTS**

MEETINGS OF INTEREST			
DATE	**LOCATIONS**	**WEBSITE**	**TITLE**
April 7–12, 2019	Vienna, Austria	https://www.egu.eu	EGU
May 26–30, 2019	Makuhari Messe,Chiba,Japan	http://www.jpgu.org/meeting_e2019/	JpGU Meeting
June 3–5, 2019	Voss,Norway	http://www.iris.no/enkf/enkf-homepage	14th International EnKF workshop
July 28–August 2, 2019	Singapore	http://www.asiaoceania.org/aogs2019/public.asp?page=home.htm	16th Annual Meeting Asia Oceania Geosciences Society (AOGS)
July 28–August ,2 2019	Yokohama Japan	https://igarss2019.org/default.asp	IGARSS
September 28–October 4, 2019	Boston, MA	https://www.ametsoc.org/index.cfm/ams/meetings-events/ams-meetings/2019-joint-satellite-conference/2019-joint-satellite-conference-call-for-papers/?utm_source=Subscribers&utm_medium=Email&utm_campaign=Newsletter&zs=5EW4e1&_zl=cf3a5	Joint AMS/EUMETSAT/NOAA conference
October 31–November 6	Saint-Saveur, Québec, Canada	https://cimss.ssec.wisc.edu/itwg/index.html	TOVS ITSC THE 22nd INTERNATIONAL TOVS STUDY CONFERENCE (ITSC-22)
November 4–8, 2019	Herzliya, Israel	http://www.cospar2019.org/	4th COPSAR Symposium Small satellites for sustainable Science and Development
December 9–13, 2019	San Francisco, California	https://sites.agu.org/	AGU
January 12–16, 2020	Boston, MA	https://www.ametsoc.org/index.cfm/ams/	AMS Annual Meeting
June 2020	Fort Collins, Colorado	TBD	8th International Symposium on Data Assimilation (ISDA)

MEETINGS AND EVENTS SPONSORED BY JCSDA			
DATE	**LOCATIONS**	**WEBSITE**	**TITLE**
April 29–May 3, 2019	Beijing, China		Joint ECMWF/JCSDA/CMA Radiative Transfer Workshop
May 29–31, 2019	NASA Headquarters		2019 17th Annual JCSDA Science and Technical Workshop
May or June 2019 (proposed)	Boulder, CO		JEDI Academy 3
October 2019 (proposed)	Monterey, CA (proposed)		JEDI Academy 4

CAREER OPPORTUNITIES

The Joint Center for Satellite Data Assimilation is currently seeking qualified candidates to fill several varied job openings. Descriptions of these positions and directions for applying may be found via the University Corporation for Atmospheric Research the Cooperative Programs for the Advancement of Earth System Science (UCAR/CPAESS) webpage: https://cpaess.ucar.edu/employment-announcements.

JOB TITLE	LOCATION
JCSDA Associate Scientist III - NIO UFO (19112)	Boulder, Colorado, United States
JCSDA Software Engineer II - PyOOPS (19104)	Boulder, Colorado, United States
JCSDA Associate Scientist III - NIO UFO (19112)	Various, United States
JCSDA Project Scientist I - IOS FSOI (19110)	Various, United States
JCSDA Project Scientist I - NIO GIIRS (19116)	Madison, Wisconsin, United States
JCSDA Project Scientist I/II - EMC Liaison (19105)	College Park, Maryland, United States
JCSDA Project Scientist I/II - ESRL Liaison (19107)	Boulder, Colorado, United States
JCSDA Project Scientist I/II - NIO RadDA (19111)	College Park, Maryland, United States
JCSDA Project Scientist II - LandDA (19113)	Various, United States

For a full listing of job openings available for NCAR/UCAR, please visit this website.

Opportunities in support of JCSDA may also be found at http://www.jcsda.noaa.gov/careers.php as they become available.